NATIONAL ADVISORY COMMITTEE
FOR AERONAUTICS

TECHNICAL NOTE 3228

AERODYNAMIC INVESTIGATION OF A FOUR-BLADE PROPELLER

OPERATING THROUGH AN ANGLE-OF-ATTACK

RANGE FROM 0° TO 180°

By H. Clyde McLemore and Michael D. Cannon

Langley Aeronautical Laboratory
Langley Field, Va.

NACA

Washington
June 1954

AFMDC
TECH

NATIONAL ADVISORY COMMITTEE FOR AERONAUTICS

TECHNICAL NOTE 3228

AERODYNAMIC INVESTIGATION OF A FOUR-BLADE PROPELLER

OPERATING THROUGH AN ANGLE-OF-ATTACK

RANGE FROM 0° TO 180°

By H. Clyde McLemore and Michael D. Cannon

SUMMARY

An investigation of the aerodynamic characteristics of a four-blade rigid model propeller has been conducted in the Langley full-scale tunnel for angles of attack from 0° to 180°, blade angles from 0° to 67.5°, and a range of advance ratio from 0 to 6.2. The investigation included a preliminary exploration of vertical descent and a comparison with theory of the rate of change of the normal-force coefficient with angle of attack and of the aerodynamic characteristics of the propeller at zero angle of attack.

The static-thrust results indicate that the blade angle for the maximum figure of merit is slightly greater than 8°. The blade angle for maximum efficiency for forward flight at zero angle of attack is approximately 60°. For the unstalled portion of the advance-ratio range investigated, thrust, power, and normal-force coefficients increase with increasing angle of attack for a given value of advance ratio and blade angle. Vertical-descent velocity should probably be limited to values removed somewhat from the slipstream velocity because of increasingly violent fluctuations of forces and moments as the descent velocity approaches the slipstream velocity in a fully developed vortex-ring state of flow at the propeller disk.

The theoretical method used for calculating the rate of change of the normal-force coefficients with angle of attack, normally applied to propellers, does not adequately predict the experimentally determined results for angles of attack greater than 15°. For the blade angles investigated, the strip-analysis theory using available two-dimensional airfoil data adequately predicted the variation of the thrust and power coefficients and efficiency with advance ratio for an angle of attack of 0°.

INTRODUCTION

The interest in propeller-driven vertically rising and descending airplanes has greatly increased the demand for information concerning the aerodynamic characteristics of propellers through a very large angle-of-attack range (0° to 180°). Propellers are known to produce a large normal force when subjected to large angles of attack, and the magnitude of this normal force and its rate of change with angle of attack, together with the moments acting on the propeller, are of primary interest to the airplane designer because of their effects on the stability and control of the aircraft.

The present tests were conducted in the Langley full-scale tunnel in order to determine the aerodynamic characteristics of a propeller while operating through an angle-of-attack range from 0° to 180° for values of advance ratio varying from 0 to 6.2. The propeller was originally designed to be used on a convertible-type airplane.

In addition to presenting the basic propeller characteristics, the paper includes a comparison with one of the available theories for several angles of attack in order to determine whether the variation of the rate of change of the normal-force coefficient with angle of attack for large angles of attack can be adequately predicted. Calculations to determine the aerodynamic characteristics of the propeller at zero angle of attack by using strip theory are also presented.

COEFFICIENTS AND SYMBOLS

The results of the tests are presented as standard NACA coefficients of forces and moments. The data are referred to a system of axes, noted in figure 1, which coincides with the propeller thrust axis and a plane perpendicular to the thrust axis and midway between the two propeller-disk planes.

T   propeller thrust, lb

N   propeller normal force, lb

Q   propeller torque, ft-lb

M   propeller pitching moment, ft-lb

Y   propeller yawing moment, ft-lb

C_T thrust coefficient, $T/\rho n^2 D^4$

C_P power coefficient, $2\pi C_Q$

C_N normal-force coefficient, $N/\rho n^2 D^4$

N_C normal-force coefficient, $\dfrac{N}{\frac{1}{2}\rho V^2 \frac{\pi D^2}{4}}$ or $\dfrac{8}{\pi}\dfrac{C_N}{J^2}$

C_Q torque coefficient, $Q/\rho n^2 D^5$

C_m pitching-moment coefficient, $M/\rho n^2 D^5$

C_Y yawing-moment coefficient, $Y/\rho n^2 D^5$

M_{tip} Mach number of propeller tip

RN Reynolds number based on chord at 0.75R station

n propeller rotational speed, rps

D propeller diameter, 5.33 ft

R propeller tip radius, 2.66 ft

ρ mass density of air, slugs/cu ft

V velocity of free-stream tunnel airstream, fps

J propeller advance ratio based on streamwise component of velocity, V/nD

J' propeller advance ratio based on velocity component normal to propeller disk, $V\cos\alpha/nD$

η propeller efficiency based on free-stream tunnel velocity, $J\dfrac{C_T}{C_P}$

r radius at any propeller blade section, ft

x fraction of propeller tip radius, r/R

B number of blades

b propeller blade chord, ft

c_e propeller equivalent chord, $\int_0^R br^2 dr \Big/ \int_0^R r^2 dr$, ft

h propeller-blade-section maximum thickness, ft

σ_e weighted propeller solidity, $Bc_e/\pi R$

α angle of attack measured from propeller-shaft axis to longitudinal tunnel axis, deg

ψ angle of attack measured from propeller-shaft axis to longitudinal tunnel axis, radians

β propeller blade angle measured at 0.75R, deg

θ propeller blade angle measured at any radius, deg

c_{l_d} propeller-blade design section lift coefficient

N_{C_ψ} rate of change of propeller normal-force coefficient with angle of attack per radian, $\partial N_C/\partial \psi$

MODEL AND APPARATUS

The propeller configuration tested was a 1/3-scale model of a propeller (design $J = 4.0$) designed for use on a convertible-type airplane, which was used previously for the investigations reported in references 1 and 2. The propeller configuration consisted of two, two-blade, 5.33-foot-diameter propellers mounted in tandem so as to form a four-blade configuration having a solidity of 0.121 based on the chord at the 0.75R station, a weighted solidity of 0.159 based on equivalent chord c_e, and an activity factor of 90.3. These tandem propellers were mounted in the same hub and rotated in the same direction. The amount of offset of the propellers is 0.35 foot. The propellers were designed to flap ±10° in a forward and rearward plane; but for the present tests, the blades were locked in a rigid position. The blades were constructed of steel and duralumin. Calculations were made of the torsional deflection under load and found to be negligible. Blade-form curves for the test propeller having NACA 16-series sections are given in figure 2.

A photograph showing the propeller mounted for tests in the Langley full-scale tunnel is given in figure 3. Power was supplied to the propeller through a right-angle gear box by a 200-horsepower electric-induction motor mounted vertically in the propeller test tower. A

schematic drawing of the tower with all pertinent components and dimensions is presented in figure 4. The tower was designed to pivot about its vertical axis; thus an unlimited angle-of-attack range was provided. Angle of attack for the present tests is considered to be in a horizontal plane. The tower support structure was shielded from the tunnel airstream by a free-floating fairing attached at its base to a rigid 1/4-inch steel plate which served as a support and turntable for the fairing. The tower was mounted on a shielded strut that transmitted the forces acting on the propeller to the tunnel balance system. In addition to the forces measured on the balance system, forces and moments acting on the propeller were determined by a calibrated strain-gage balance mounted integrally with the structure of the tower (fig. 4). The propeller, gear box, and motor were mounted on a rigid frame pivoted on gimbals which allowed freedom of movement only in the thrust and normal-force directions. The frame was restrained from pivoting in the gimbals by the strain-gage beams. Propeller torque was measured by a strain-gage beam attached to the drive motor. The tail boom was used to counterbalance the static load on the thrust strain gages caused by the weight of the propeller and hub mechanism.

TESTS

Tests at static thrust were conducted in the Langley full-scale-tunnel hangar (which is a large, unobstructed room) with the propeller slipstream directed through the opened hangar doors. These tests were made for a range of blade angle varying from 0° to 25° for several values of propeller rotational speed with the limiting condition being the maximum allowable rotational speed as limited by available torque. The thrust and torque were measured by a calibrated strain-gage system.

Tunnel-operating force tests were made of the propeller for a range of angle of attack from 0° to 180°. These angles of attack were obtained by rotating the tower in a horizontal plane through approximately 90° for the forward-flight tests. However, to avoid the gross tower-wake-interference effects expected for angles of attack greater than 90°, the tower angles of attack were decreased toward $\alpha = 0°$ with the propeller pitch angles and propeller rotation reversed so that the free-stream air approached the propeller disk from the rear. At nearly every angle of attack investigated, several propeller blade angles were tested which, from preliminary calculations, seemed appropriate. Blade angles, measured at 0.75R, varied from 0° to 67.5° with J' varying from 0 to 6.2. Maximum tunnel velocity of the tests was 140 fps, corresponding to a tunnel Mach number of 0.12, and the maximum tip speed was 697 fps, corresponding to a tip Mach number of 0.62.

Each tunnel test condition consisted of setting a predetermined angle of attack and blade angle with propeller rotational speed and tunnel airspeed varied to give a maximum range of advance ratio. The airspeeds below about 30 fps could not be obtained under steady conditions because of the lower operating limit of the tunnel drive motors. These speeds were obtained under transient conditions in which the tunnel motors were turned off and the data were taken at time intervals of 20, 40, and 70 seconds after shutdown. These time intervals correspond to airspeeds of approximately 20, 15, and 10 fps, respectively. A calibrated propeller-type directional anemometer mounted in the tunnel was used in measuring these low airspeeds.

The force data presented for the tunnel operating conditions were obtained from wind-tunnel balance data only with the strain-gage data being used to show the magnitude and frequency of the fluctuations of the forces and moments noted for the vertical descent tests. The strain-gage system was a moment-measuring system and, therefore, could be used to obtain only force results at static thrust or very low advance ratios or for very low angles of attack. Torque was measured by a strain gage attached to the drive motor.

Visual and photographic observations were made of a limited smoke study of the propeller in a near vertical descent condition for an angle of attack of 165° and a blade angle of 16°.

RESULTS AND DISCUSSION

Presentation of Results

The results of the present investigation are grouped into four main sections. The first section includes the static-thrust characteristics for a range of propeller blade angle from 0° to 25°. The results of this section are given in figures 5 and 6. The second section presents the aerodynamic characteristics of the propeller for a very large angle-of-attack range (0° to 82.5°), a range of J' from 0 to 6.2, and with the blade angles varying from 4° to 67.5°. These results are presented in figures 7 to 13.

The third section deals with the aerodynamic characteristics of the propeller when the relative wind is into the rear side of the propeller disk simulating a condition of airplane tail-first descent. The results of this section are presented in figures 14 to 18. The final section presents a comparison with theory of the variation of the rate of change of the propeller normal-force coefficient with angle of attack. A comparison with theory of the experimentally determined values of C_T, C_P, and η was also made for an angle of attack of 0°. The results of this section are presented in figures 19 and 20.

The data have been corrected for tunnel blockage, propeller-removed tares, and gear-box losses. In connection with the gear-box losses, it is important to state that gearing failures occurred twice during the course of the tests, and the second failure caused a slight curtailment of the original test program. Since it was necessary to assemble the gear box a third time, reworked gears were used in order to obtain the tare torque due to gearing with the propeller removed. Some inaccuracy in the power measurements, therefore, is to be expected. It was not feasible to make periodic checks of the tare torque during the course of the tests, but comparisons of the calculated propeller characteristics at $\alpha = 0^{\circ}$, by use of strip theory, with the experimentally derived characteristics (fig. 20) show fair agreement, as will be more fully discussed later. In regard to the accuracy, however, it is usually possible to predict peak propeller efficiencies to within ±3 percent by strip-theory methods, whereas the results in figure 20(c) show differences as high as 5 percent. Some of this difference may be due to inaccuracies in the measurement of the power delivered to the propeller.

No corrections have been made for jet-boundary effects or for the local stream angle at the propeller. The former are known to be very small because of the small propeller size used in the Langley full-scale tunnel. With regard to the stream angle, the normal force measured at a nominal propeller angle of attack of 0° indicates that the propeller actually has an initial angle of attack of approximately -2° or -3°. Inasmuch as the propeller location in the tunnel changes with each angle-of-attack setting, the work involved in obtaining the airstream surveys required to define accurately the stream-angle variation was not felt to be warranted.

The accuracy of the force and moment data is believed to be within the following limits:

$$C_T \quad \ldots \ldots \ldots \ldots \ldots \ldots \ldots \ldots \ldots \ldots \ldots \ldots \ldots \quad \pm 0.002$$

$$C_P \quad \ldots \ldots \ldots \ldots \ldots \ldots \ldots \ldots \ldots \ldots \ldots \ldots \ldots \quad \pm 0.01$$

$$C_N \quad \ldots \ldots \ldots \ldots \ldots \ldots \ldots \ldots \ldots \ldots \ldots \ldots \ldots \quad \pm 0.01$$

$$C_Y \quad \ldots \ldots \ldots \ldots \ldots \ldots \ldots \ldots \ldots \ldots \ldots \ldots \ldots \quad \pm 0.01$$

$$C_m \quad \ldots \ldots \ldots \ldots \ldots \ldots \ldots \ldots \ldots \ldots \ldots \ldots \ldots \quad \pm 0.01$$

Static Thrust

Each static-thrust test was made with a fixed blade angle; therefore, changes in propeller characteristics during a test are due only to changes in rotational speed. The variation of thrust and power coefficients with

Reynolds number and tip Mach number for a range of blade angle from 0°
to 25° are given in figure 5. In general, the C_T and C_P curves are
consistent with the trends obtained for most propellers in static thrust,
and a detailed discussion of figure 5 is felt to be unnecessary.

The propeller figure of merit $0.798 \dfrac{C_T^{3/2}}{C_P}$, which is the ratio of
the ideal minimum power required to produce a given thrust to the actual
power required to produce the same thrust, plotted against the ratio of
thrust coefficient to weighted solidity C_T/σ_e for the range of tip Mach
number, Reynolds number, and blade angle investigated is given in fig-
ure 6. The blade angle for the maximum figure of merit is slightly
greater than 8°. For values of C_T/σ_e up to about 1.1, the figure of
merit is seen to increase rapidly at first and then more slowly with
increasing Reynolds number and tip Mach number. At values of C_T/σ_e in
excess of 1.1, the figure of merit at the higher Reynolds numbers and
tip Mach numbers shows a reduction with increasing Reynolds number and
tip Mach number. This drop in the figure of merit may be a compressibil-
ity effect in view of the well-known fact that the critical Mach number
of airfoil sections decreases with increasing angle of attack (ref. 3).

Forward Flight

The forward-flight regime for a vertically rising airplane could
conceivably include angles of attack varying from 0° to approximately 90°.
The very high angle-of-attack range would probably be attained only at
very low values of J' representing a very slow forward speed at take-
off and landing or in the transition flight range. Of course, at high
altitude during maneuvers, an airplane configuration could attain fairly
high angles of attack at considerably higher values of J' than the
take-off condition; therefore, the present tests were conducted to include
a very large J' range over the large angle-of-attack range to include
all possible flight conditions which this type airplane may experience,
including airplane configurations having capabilities of a wide range of
propeller speed by variable gear ratios.

The aerodynamic characteristics of the propeller for angles of
attack from 0° to 82.5° are presented in figures 7 to 13. The blade
angle for this range of angle of attack was varied from 30° to 67.5°
at $\alpha = 0^\circ$ and from 4° to 30° at $\alpha = 82.5^\circ$. The coefficients presented
in these figures are C_T, C_P, C_N, C_Y, and C_m and are plotted against
J'. The propeller efficiency (fig. 7(c)) is shown for $\alpha = 0^\circ$ only.

The value of J' giving zero thrust for a given blade angle increased
with increasing angle of attack for the blade angle and J' range inves-
tigated (figs. 7 to 13). Except for the stalled range at low J', the
values of C_T at a given blade angle increased with increasing angle of
attack until the very high angles of attack were reached. For angles of
attack of 75° and 82.5°, the higher blade angles tested gave decreased
values of C_T with increasing J' for the higher J' range investi-
gated. This fact indicates that the optimum blade angle for producing
a net thrust has been exceeded. These angles of attack of 75° and greater
are in a range that is synonymous with helicopter forward flight and the
data would no longer be expected to follow the trend of normal propeller
operation. A preliminary calculation, using the method of reference 4, of
the section angles of attack about the disk for these very large propeller
angles of attack showed an increase in section angle of attack on the
forward-going blade and a decrease in section angle of attack on the
rearward-going blade. This blade-angle-of-attack variation plus the
effect of changing dynamic pressure on the forward- and rearward-going
blades would be expected to produce large variations in the loading over
the disk.

An attempt was made to make a more detailed calculation of the thrust
coefficients of the propeller for an angle of attack of 75° and a blade
angle of 40° for J' = 0.4 by using strip theory and the method of ref-
erence 4. For the low angle-of-attack range, section data were obtained
from reference 3; however, very large positive and negative section angles
of attack were encountered (-100° to 40°) which required the use of sec-
tion data in a range where little information is available for the present
NACA 16-series airfoil section. Therefore, an extrapolated lift curve was
determined, based on NACA 0012-series airfoil sections and Clark Y data
(refs. 5 and 6) and several thrust coefficients were calculated and found
to underestimate the experimental results by as much as 50 percent.
Inspection of the calculations showed that deviations from the extrapo-
lated curve could produce large differences in the final coefficients,
emphasizing the need for airfoil data at very large angles of attack.

The calculations did show, however, that a large portion of the disk
is operating in a region of negative thrust for the value of J' inves-
tigated, with the negative thrust condition becoming more pronounced with
increasing J'. The lack of surveys in the propeller plane or sufficient
data to define accurately the loading over the disk makes the interpreta-
tion of the thrust- and power-coefficient curves for angles of attack of
75° and 82.5° very difficult; and for the present paper, no attempt will
be made to explain the variations of C_T and C_P against J' for these
angles of attack.

The power coefficients and the normal-force coefficients for a given
blade angle and J' increase with increasing angle of attack for the
range of blade angle and J' investigated.

The blade angle for maximum efficiency at zero angle of attack is 60° at J' = 3.7.

The pitching-moment and yawing-moment coefficients, in general, increased with increasing J' and angle of attack for a given blade angle; however, no consistent trend was noted.

The side force was measured and found to be negligible and is not included in the present paper. In the case of two-blade propellers, however, it is known that the side force is of considerable magnitude. (See ref. 7.)

Vertical Descent

The flight regime for a vertically rising airplane will probably include angles of attack up to 180° which represents a tail-first vertical-descent condition. For this reason an attempt was made to determine the propeller characteristics for the very high angle-of-attack range and for a limited range of negative J' and blade angles. As suggested by the results of previous tests with this propeller installed on a model airplane configuration (reported in ref. 2) there was evidence that violent, unstable motions of that model in a tail-first condition could be attributed to the unsteady propeller slipstream. This conclusion was supported by the fact that, with the propellers removed from the model, no unstable motions of any kind were experienced at an angle of attack of 180°. The present tests with propeller alone indicated the same type of motions of approximately the same magnitude as those noted in reference 2. As in the tests of reference 2, the present simulated vertical-descent tests were limited and were terminated before any appreciable amount of data could be obtained because of the excessive wear and damage to the blades and experimental hub mechanism.

The vertical-descent tests were made by operating the tunnel at its lowest continuous velocity (V ≈ 38 fps) and varying J' by increasing the propeller rotational speed. This type of operation would allow the negative advance ratio to vary from a value of approximately -1.0 to values approaching zero (static thrust). The tests had to be terminated, however, just as the important operating range of J' (0 to -0.2) was approached. This situation was unfortunate because the operating range of the propeller of a vertically descending airplane would probably include very high rotational speeds and low descent velocities which would necessarily result in values of J' approaching zero. The accompanying aerodynamic data given in figure 14 are, therefore, of limited value except to correlate the results given in figures 15 to 18 which show the time history of the propeller thrust, normal force, and torque for the range of J' investigated. These time-history data were obtained by recording the results obtained from the strain-gage system noted in figure 4.

The time-history data (figs. 15 to 18) show the increase in magnitude of the force and moment fluctuations as J' approached zero. For the least negative values of J' investigated for each of the test conditions, the forces and moments varied as much as ±20 percent of the total values measured.

In addition to the obvious structural and fatigue problems, operation in this range would probably impair the ability to control the aircraft because of the violent flow fluctuations.

The reason for the violent fluctuations of the forces and moments is probably due to the fact that the slipstream velocity was approaching or was equal to the free-stream velocity, resulting in a very unstable region of air at the propeller disk that could be described as a fully developed vortex-ring state of flow. This flow condition has been experienced by helicopters in partial-power descents. Any descent velocity which is removed somewhat from the slipstream velocity probably will produce less violent motions.

Visual and photographic observations were made of the flow in the region of the propeller by using smoke for an angle of attack of 165°, a blade angle of 16°, and J' of approximately -0.3. The results of these observations showed a semiperiodic flow back and forth through the propeller disk, which would account for the large fluctuations in forces noted previously.

As an illustration of the magnitude of this disturbance, the anemometer located some 18 feet from the propeller (see fig. 3) was periodically turned 180° from its usual direction.

Comparison With Theory

For conventional propeller operation, Goldstein's propeller vortex theory in conjunction with two-dimensional airfoil data has been found to be a reliable method of predicting the aerodynamic characteristics of propellers. (See ref. 8.) In application to yawed or pitched propeller problems, except for small angles of pitch or yaw, this method has so far been handicapped by a lack of two-dimensional airfoil data at high angles of attack, as has already been mentioned earlier in the present paper. Actually, of course, it is not certain whether the vortex theory as now used would apply to large angles of attack or to stalled operating conditions, even if the two-dimensional airfoil data were available.

Because of the labor involved in applying strip-theory methods to the calculation of the propeller normal force for even small angles of attack, several simplified methods for calculating the normal force have been developed, the most widely used method being that of Ribner (ref. 9).

The development of this method, which is explained in reference 10, is based on the assumption of only small changes in the propeller velocity field. In application, this method has been found to give fairly reliable results for angles of attack up to approximately 15°. Use is made of the present data to check the applicability of Ribner's method over a larger range of pitch angle than previously tried.

The results of the experimentally determined values of the rate of change of the propeller normal-force coefficients with angle of attack for angles of attack from 0° to 82.5° and the results determined by the method of reference 9 are shown in figure 19. The values used for the spinner and sidewash factors in the theoretical calculations were 1.14 and 0.4, respectively, and are sufficiently accurate as determined in reference 4.

In the unstalled range of J (J > 1.8) for angles of attack of 0° and 15° and blade angles from 40° to 60°, the theory gives results that are, in general, within the ±10-percent accuracy noted in reference 9; however, for angles of attack of 30° or more, the inaccuracy was increasingly greater than ±10 percent, as can be determined from the results given in figure 19.

It is interesting to note that a decrease in section lift-curve slope (which was 0.1 per degree) used in the calculations shifts the calculated curve to a lower position which is parallel to the original curve. It can be seen by inspection of figure 19 for angles of attack of 60° and 75° that, by decreasing the section lift-curve slope, the calculated curve would be shifted downward, and would result in a closer correlation of experimental and calculated results for the higher range of J investigated. It was noted that, for an angle of attack of 75°, a decrease to 0.014 per degree in the section lift-curve slope used in the theoretical method would result in a close correlation of theoretical and experimental results for J greater than 2.0. The applicable lift-curve-slope variation, however, is unknown.

The method of reference 9 gives results that fall still farther from the experimental results when angle of attack is increased to 82.5°. The experimental results show negative values of N_{C_ψ}, whereas the theoretical method used has no provision to account for these negative values.

The aerodynamic characteristics of a propeller at zero angles of attack and yaw can, in general, be adequately predicted by making use of a strip analysis for the airfoil sections used and by considering compressibility effects. This prediction was made by using available airfoil-section data (ref. 3) which were incomplete, making it necessary to rely on extrapolated values obtained from the results given in references 5 and 6 for NACA 0012-series airfoil sections and Clark Y

airfoil data, respectively. The results of these calculations, along with the experimental data, are presented in figure 20.

The variations of C_T and C_P with advance ratio are fairly well predicted by the calculations; however, the experimental data are consistently higher throughout the range tested. The variation of efficiency with J, of course, follows the trend set by the thrust and power coefficients.

The basic reason why theory does not predict the actual values of thrust and power coefficients and efficiency for the blade angles tested has not been determined. The gear-box tare torque, as discussed in the section "Presentation of Results," is a possible source for the differences in the experimental and calculated values of power coefficient and efficiency and the use of extrapolated data for portions of the calculations could also account for part of these differences. In the forward-flight section, the coefficients C_T and C_P for the unstalled range of J' are shown to increase with increasing angle of attack and it is possible that the small initial angle of attack noted in the section "Presentation of Results" is a contributing factor for the experimentally determined values being greater than theory predicts.

CONCLUSIONS

The tests of a 1/3-scale, four-blade, model propeller designed for use on a convertible-type airplane conducted in the Langley full-scale tunnel for ranges of angle of attack, blade angle, and advance ratio of $0°$ to $180°$, $0°$ to $67.5°$, and 0 to 6.2, respectively, indicate the following conclusions:

1. The blade angle for the maximum figure of merit is slightly greater than $8°$ (zero advance ratio).

2. The blade angle for maximum efficiency for zero angle of attack is approximately $60°$.

3. For the unstalled portion of the advance-ratio range, thrust, power, and normal-force coefficients increase with increasing angle of attack for a given value of advance ratio and blade angle.

4. Thrust and torque varied as much as ± 20 percent during the portion of the vertical-descent tests where the slipstream velocity approached the free-stream velocity. The strength and fatigue problems developed in the propeller due to these forces, together with the difficulties that may be experienced in controlling the aircraft because of the abrupt

slipstream fluctuations, may limit rates of descent to values somewhat removed from the slipstream velocity.

5. The theoretical method of Ribner does not adequately predict the rate of change of the normal-force coefficient with angle of attack for angles of attack greater than 15°.

6. The strip analysis carried out in an effort to predict the measured characteristics at zero angle of attack predicted fairly well the experimental results.

Langley Aeronautical Laboratory,
       National Advisory Committee for Aeronautics,
              Langley Field, Va., March 15, 1954.

REFERENCES

1. Lange, Roy H., Cocke, Bennie W., Jr., and Proterra, Anthony J.: Preliminary Full-Scale Investigation of a 1/3-Scale Model of a Convertible-Type Airplane. NACA RM L9C29, 1949.

2. Lange, Roy H., and McLemore, Huel C.: Static Longitudinal Stability and Control of a Convertible-Type Airplane As Affected by Articulated- and Rigid-Propeller Operation. NACA TN 2014, 1950. (Supersedes NACA RM L9C24.)

3. Lindsey, W. F., Stevenson, D. B., and Daley, Bernard N.: Aerodynamic Characteristics of 24 NACA 16-Series Airfoils at Mach Numbers Between 0.3 and 0.8. NACA TN 1546, 1948.

4. Crigler, John L., and Gilman, Jean, Jr.: Calculation of Aerodynamic Forces on a Propeller in Pitch or Yaw. NACA TN 2585, 1952. (Supersedes NACA RM L8K26.)

5. Jacobs, Eastman N., and Abbott, Ira H.: Airfoil Section Data Obtained in the NACA Variable-Density Tunnel As Affected by Support Interference and Other Corrections. NACA Rep. 669, 1939.

6. Knight, Montgomery, and Wenzinger, Carl J.: Wind Tunnel Tests on a Series of Wing Models Through a Large Angle of Attack Range. Part I - Force Tests. NACA Rep. 317, 1929.

7. Flachsbart, O., and Kröber, G.: Experimental Investigation of Aircraft Propellers Exposed to Oblique Air Currents. NACA TM 562, 1930.

8. Crigler, John L.: Comparison of Calculated and Experimental Propeller Characteristics for Four-, Six-, and Eight-Blade Single-Rotating Propellers. NACA WR L-362, 1944. (Formerly NACA ACR 4B04.)

9. Ribner, Herbert S.: Formulas for Propellers in Yaw and Charts of the Side-Force Derivative. NACA Rep. 819, 1945. (Supersedes NACA ARR 3E19.)

10. Ribner, Herbert S.: Propellers in Yaw. NACA Rep. 820, 1945. (Supersedes NACA ARR 3L09.)
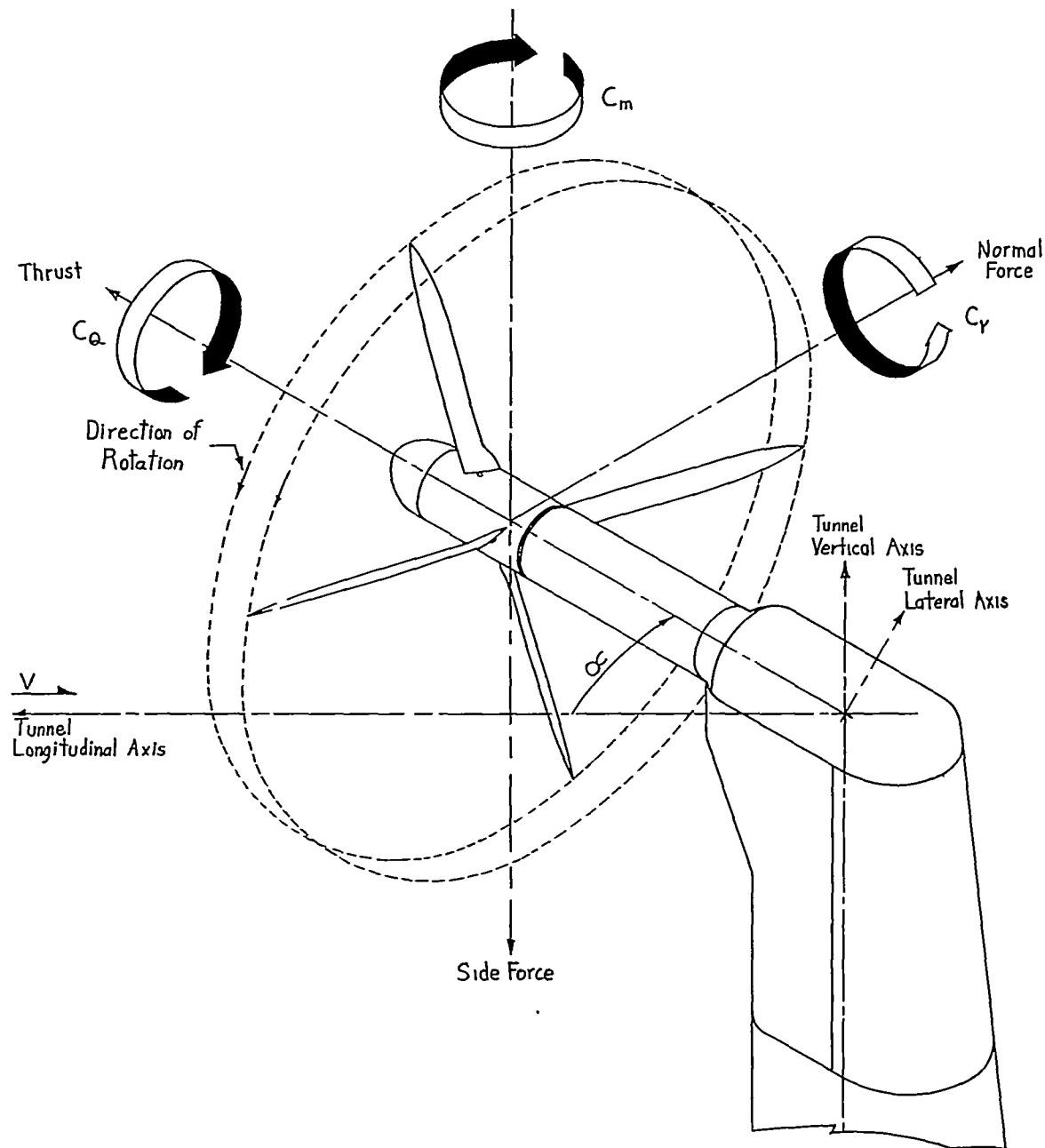
Figure 1.- System of axes used. Arrows denote positive direction of forces, moments, and angular displacements.
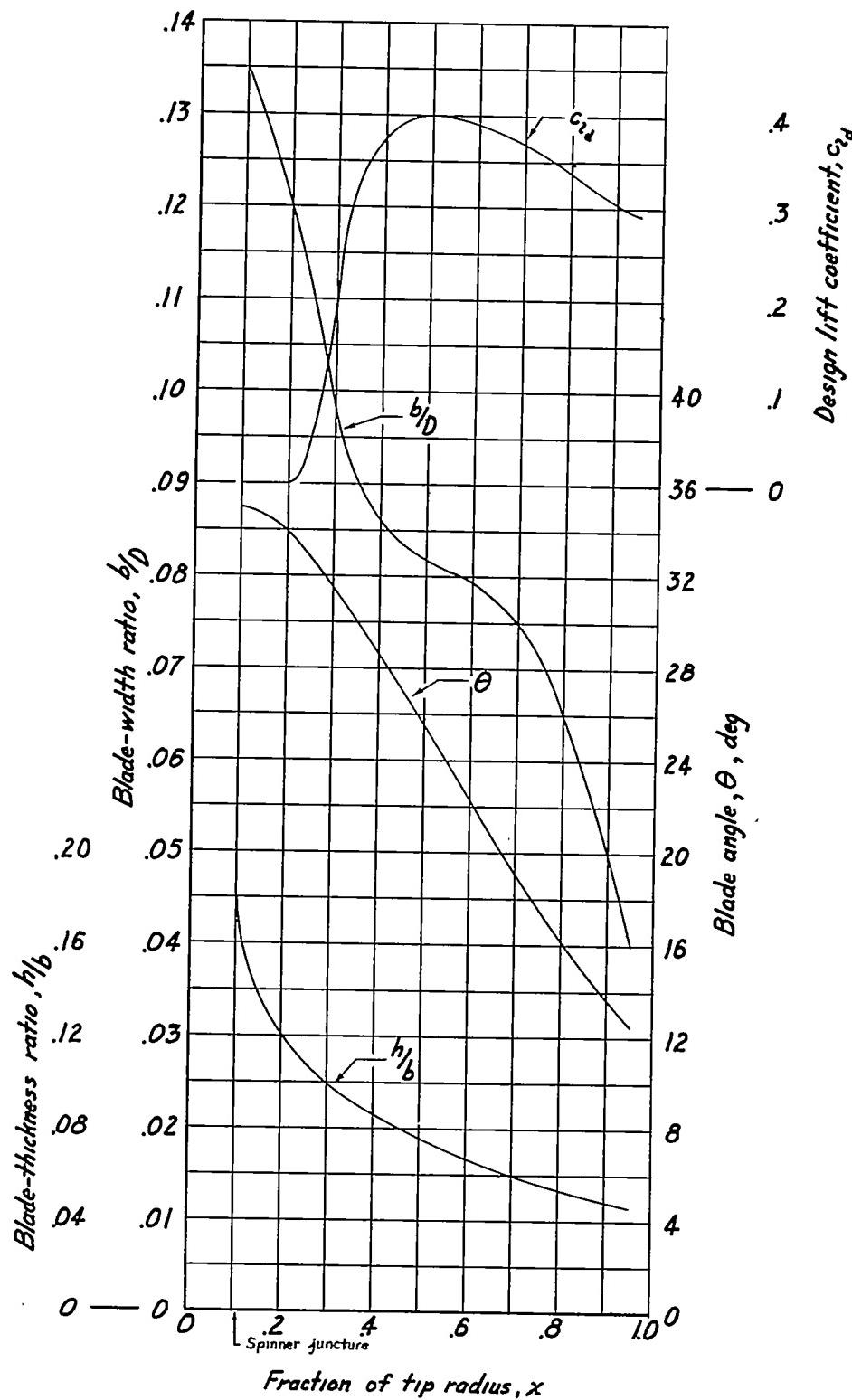
Figure 2.- Blade-form curves for propeller.
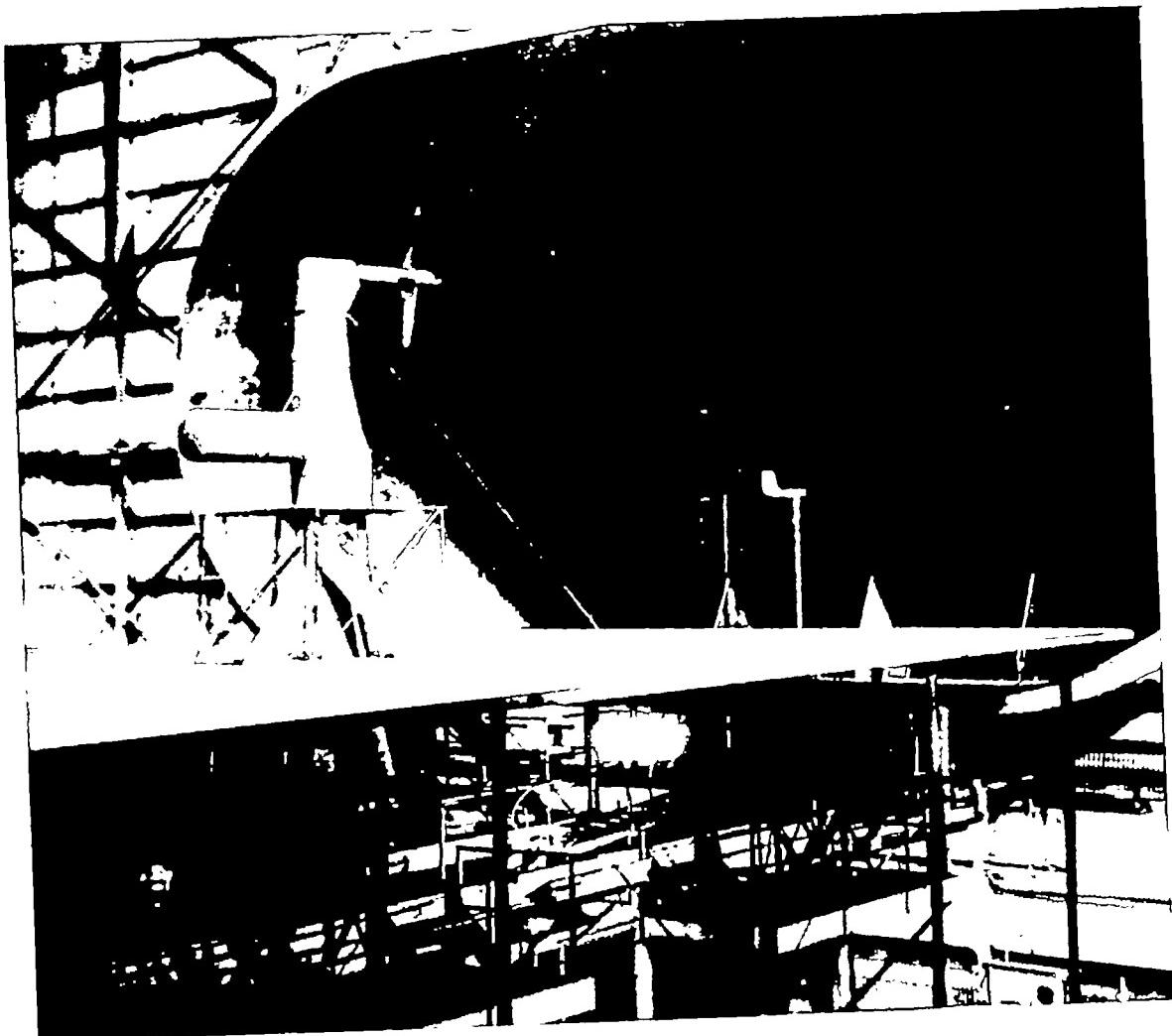
L-77492

Figure 3.- Photograph of propeller mounted for tests in Langley
full-scale tunnel.
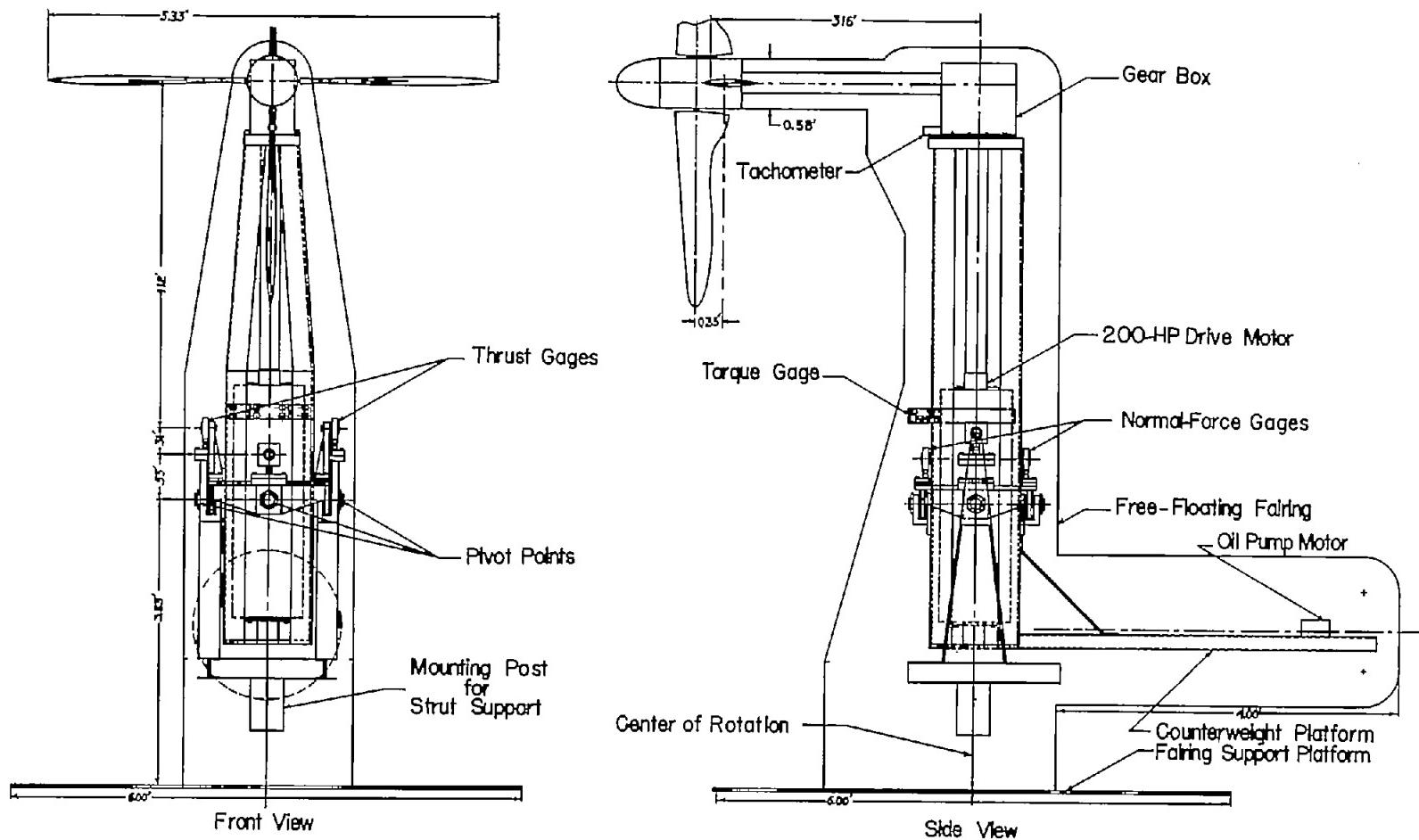
Figure 4.- Schematic drawing of propeller test tower.
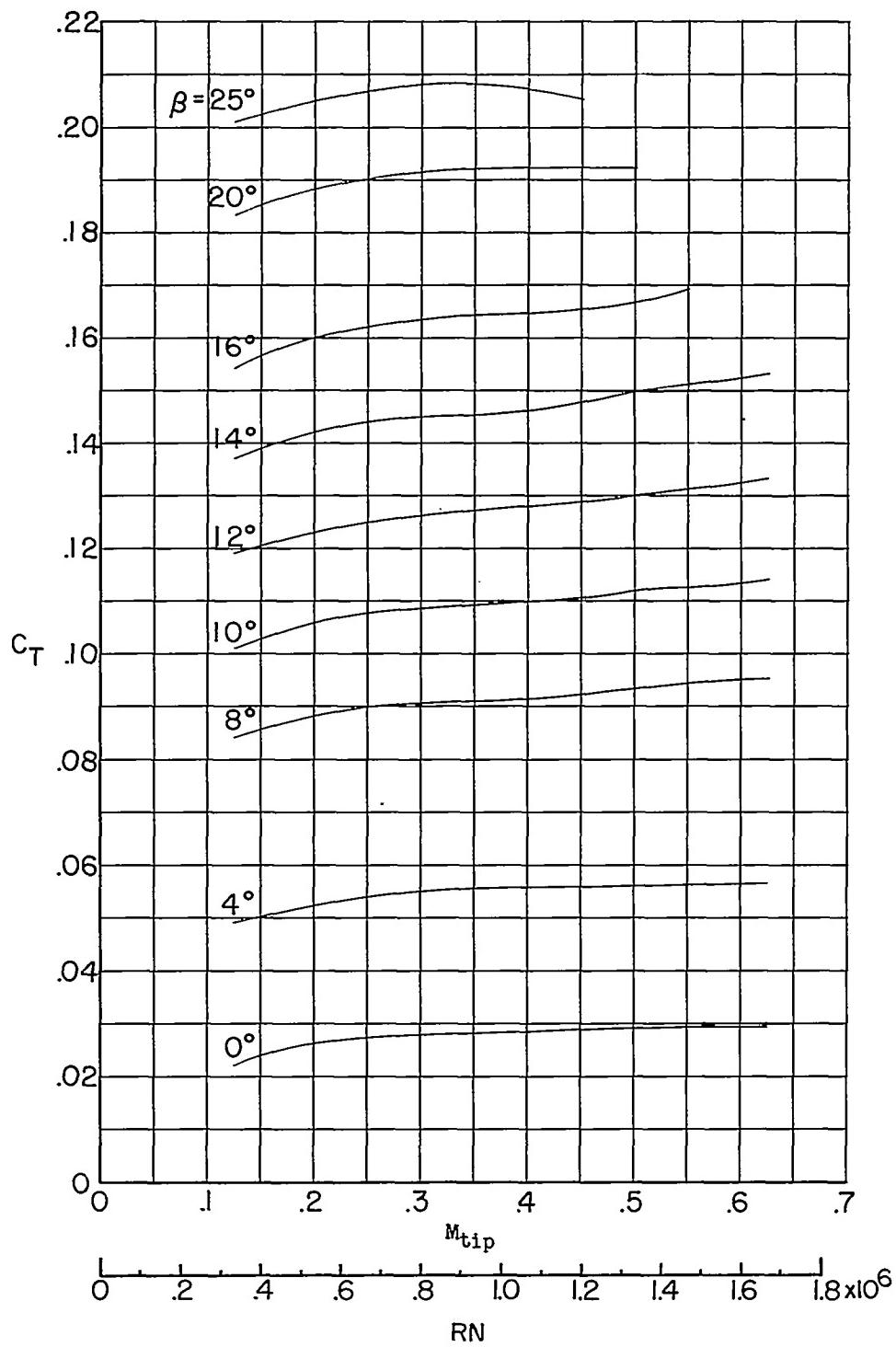
(a) C_T against M_{tip} and RN.

Figure 5.- Static-thrust characteristics for several propeller blade angles.
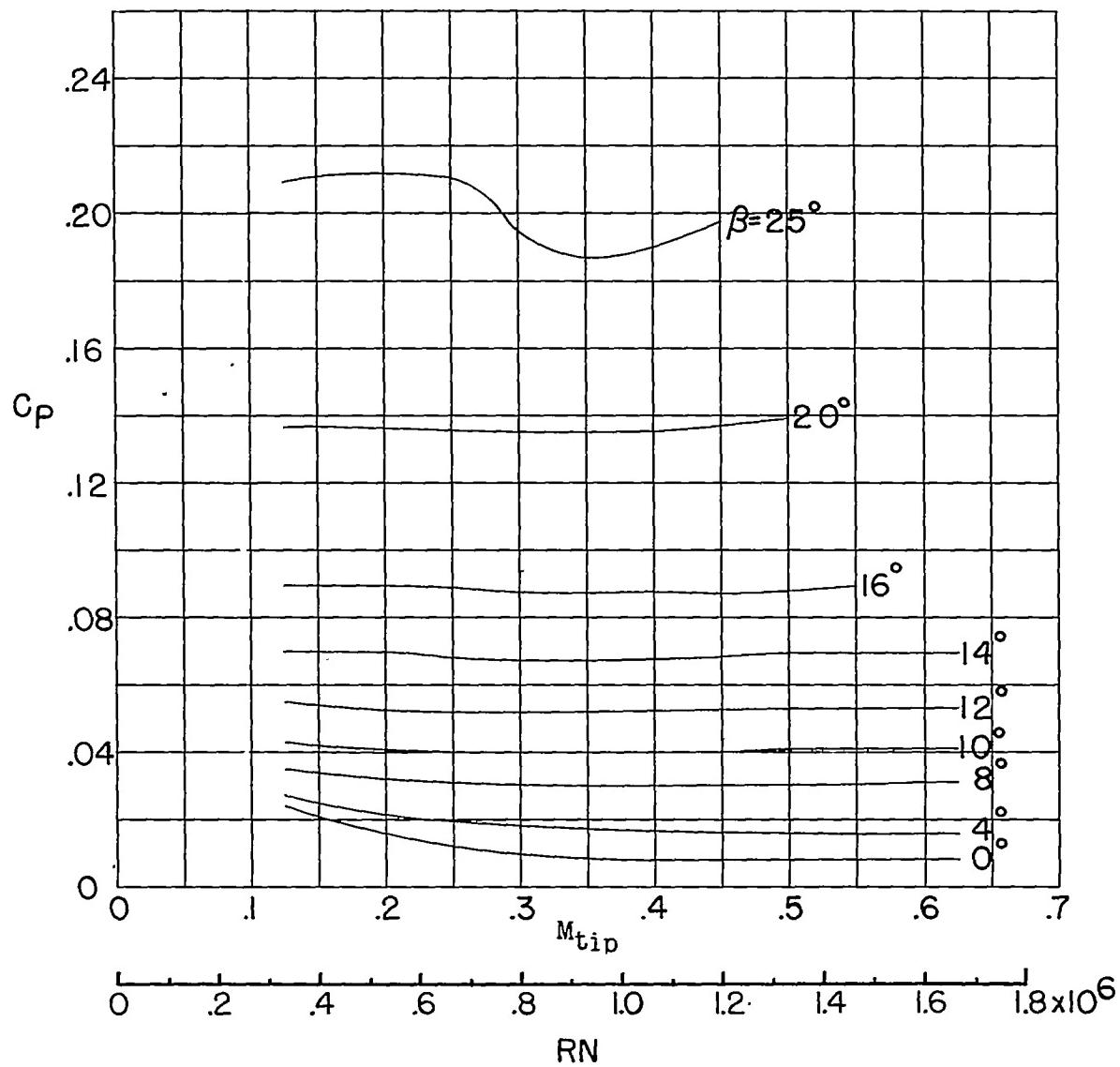
(b) C_P against M_{tip} and RN.

Figure 5.- Concluded.

Figure of Merit, $.798\ C_T^{3/2}/C_P$

C_T/σ_e

M_{tip}	RN×10⁻⁶
.625	1.667
.600	1.600
.550	1.467
.500	1.333
.450	1.200
.400	1.067
.350	.933
.300	.800
.250	.667
.200	.533
.150	.400
.125	.333
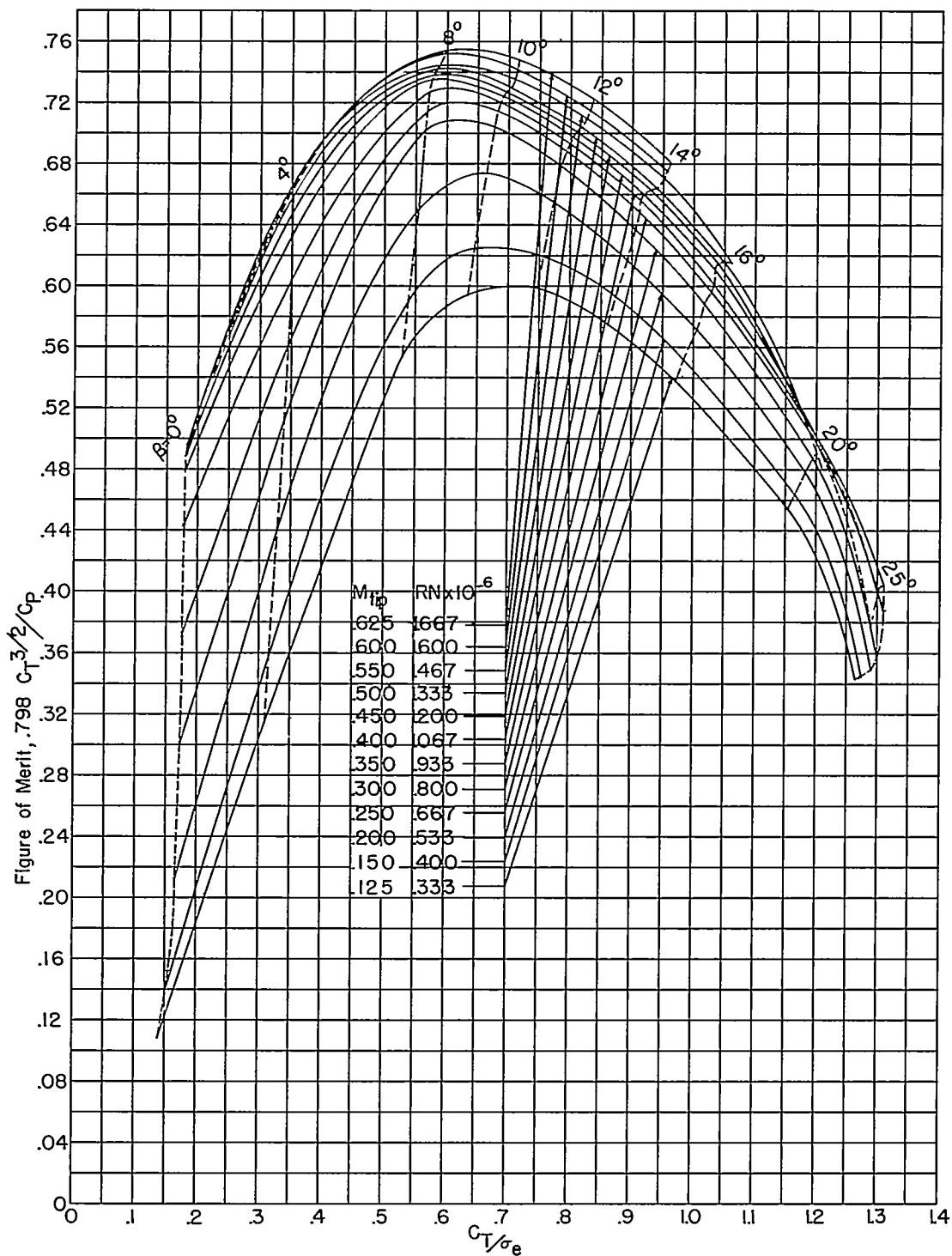
Figure 6.- Variation of propeller figure of merit against weighted thrust coefficient for several blade angles, Reynolds numbers, and tip Mach numbers.
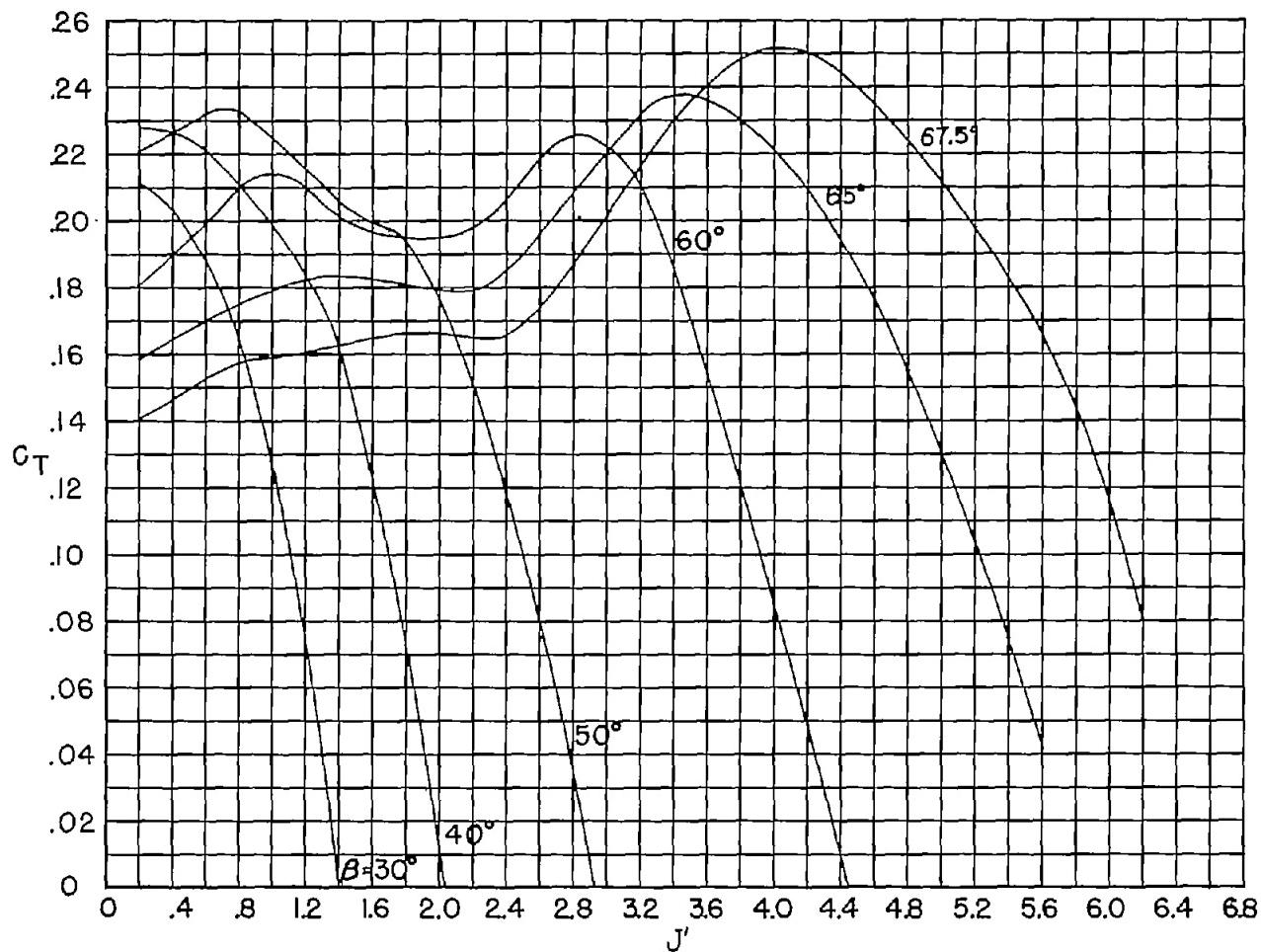
(a) C_T against J'.

Figure 7.- Variation of propeller characteristics C_T, C_P, η, C_N, C_Y, and C_m with J'. $\alpha = 0^\circ$.
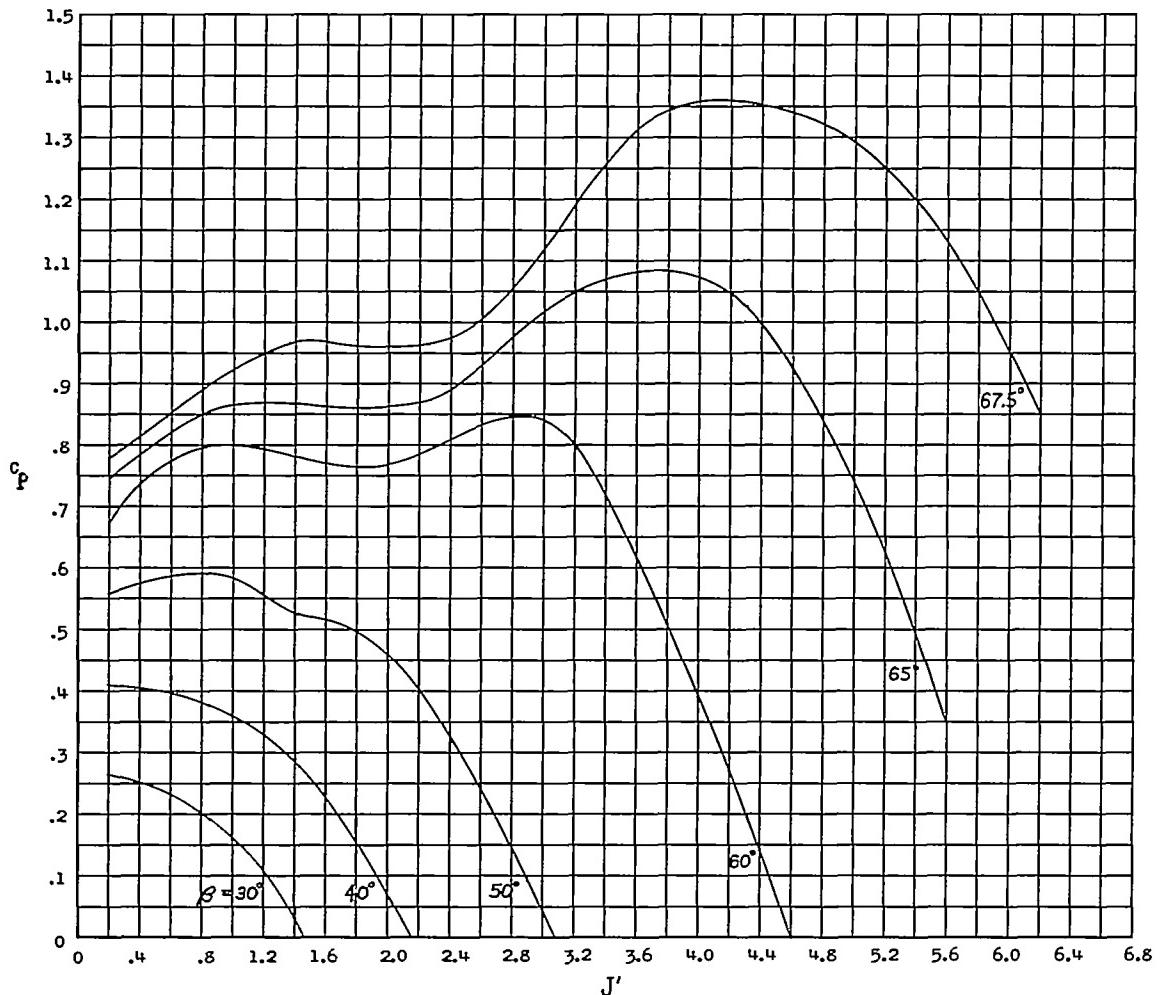
(b) C_P against J'.

Figure 7.- Continued.
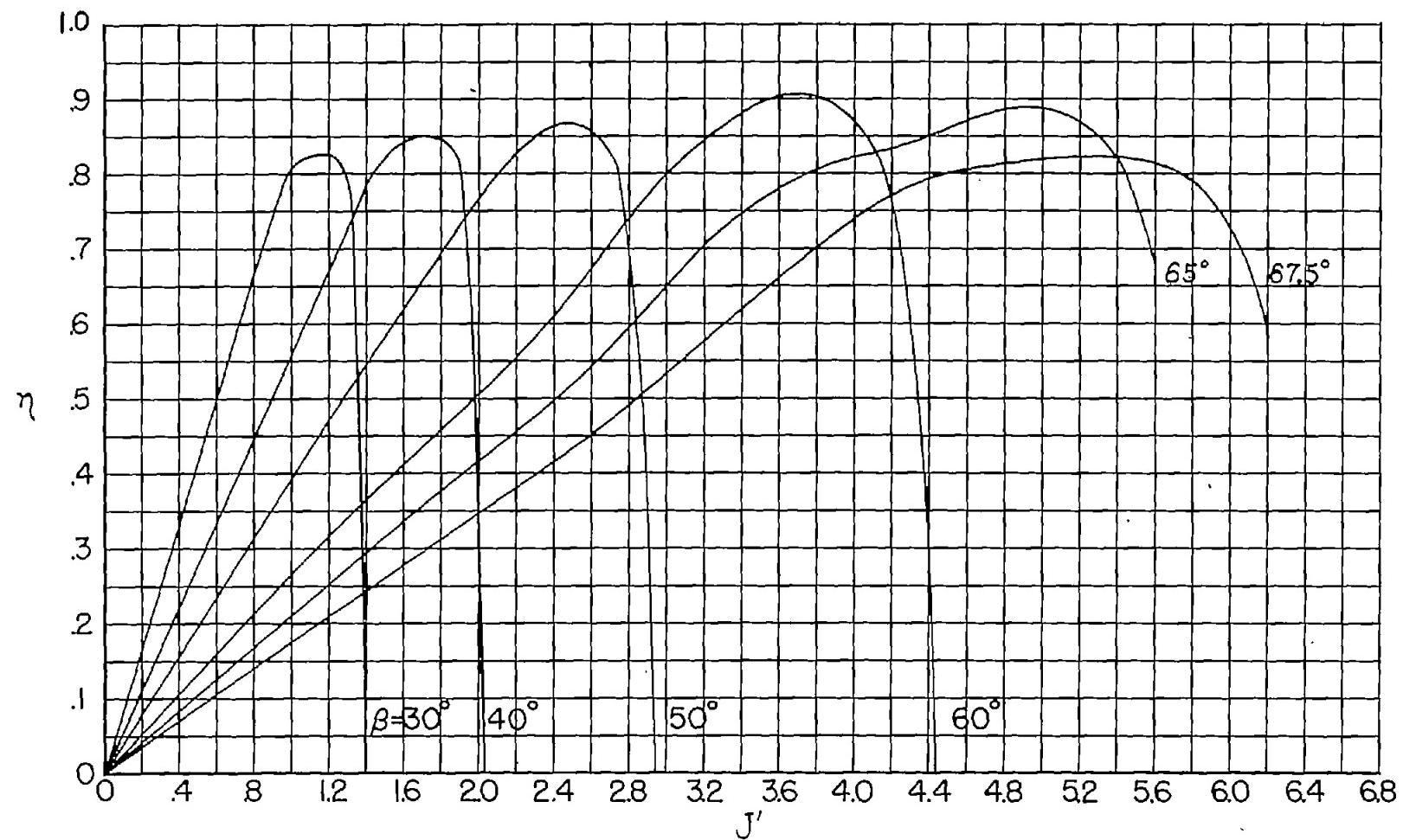
(c) η against J'.
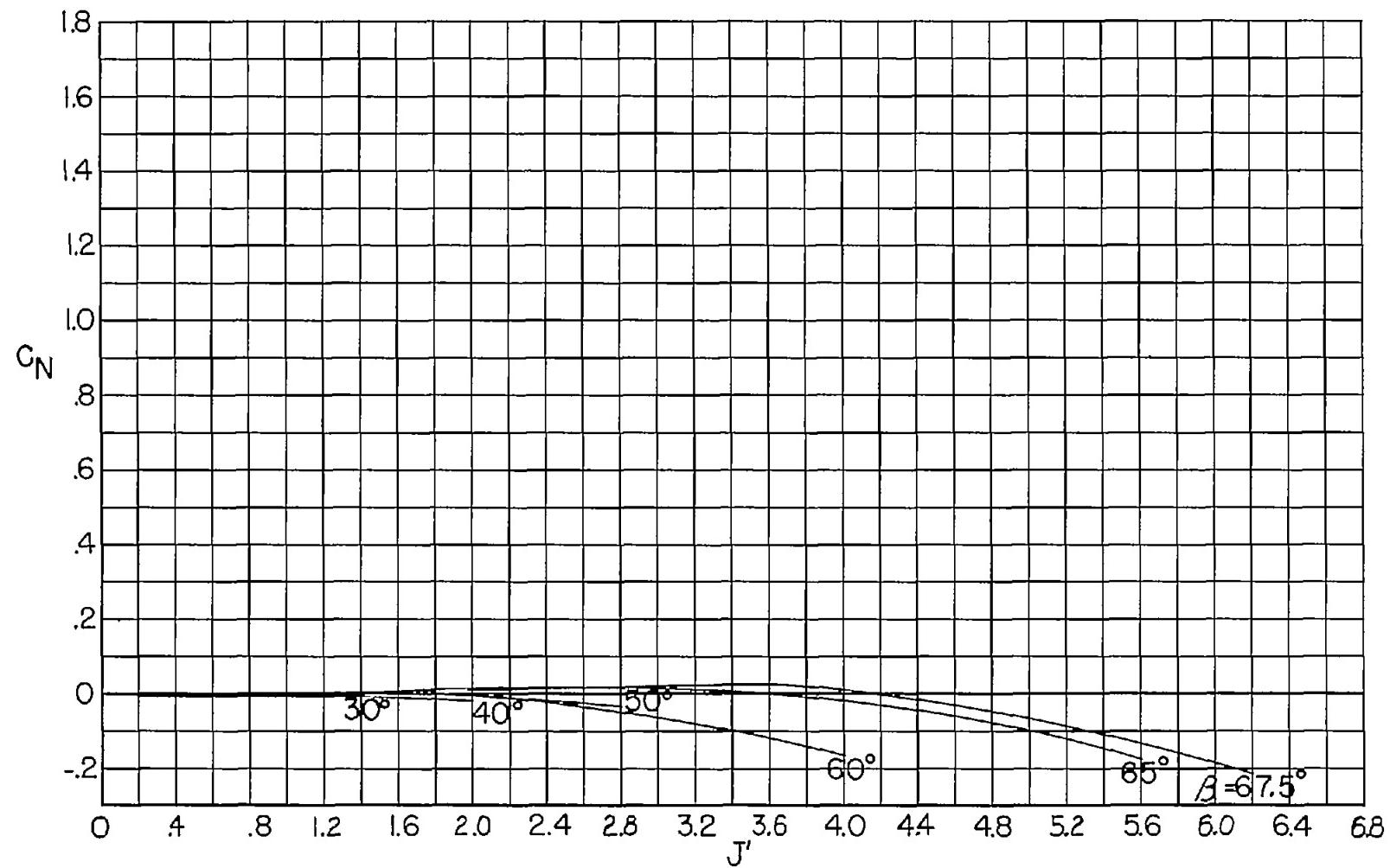
Figure 7.- Continued.

(d) C_N against J'.

Figure 7.- Continued.
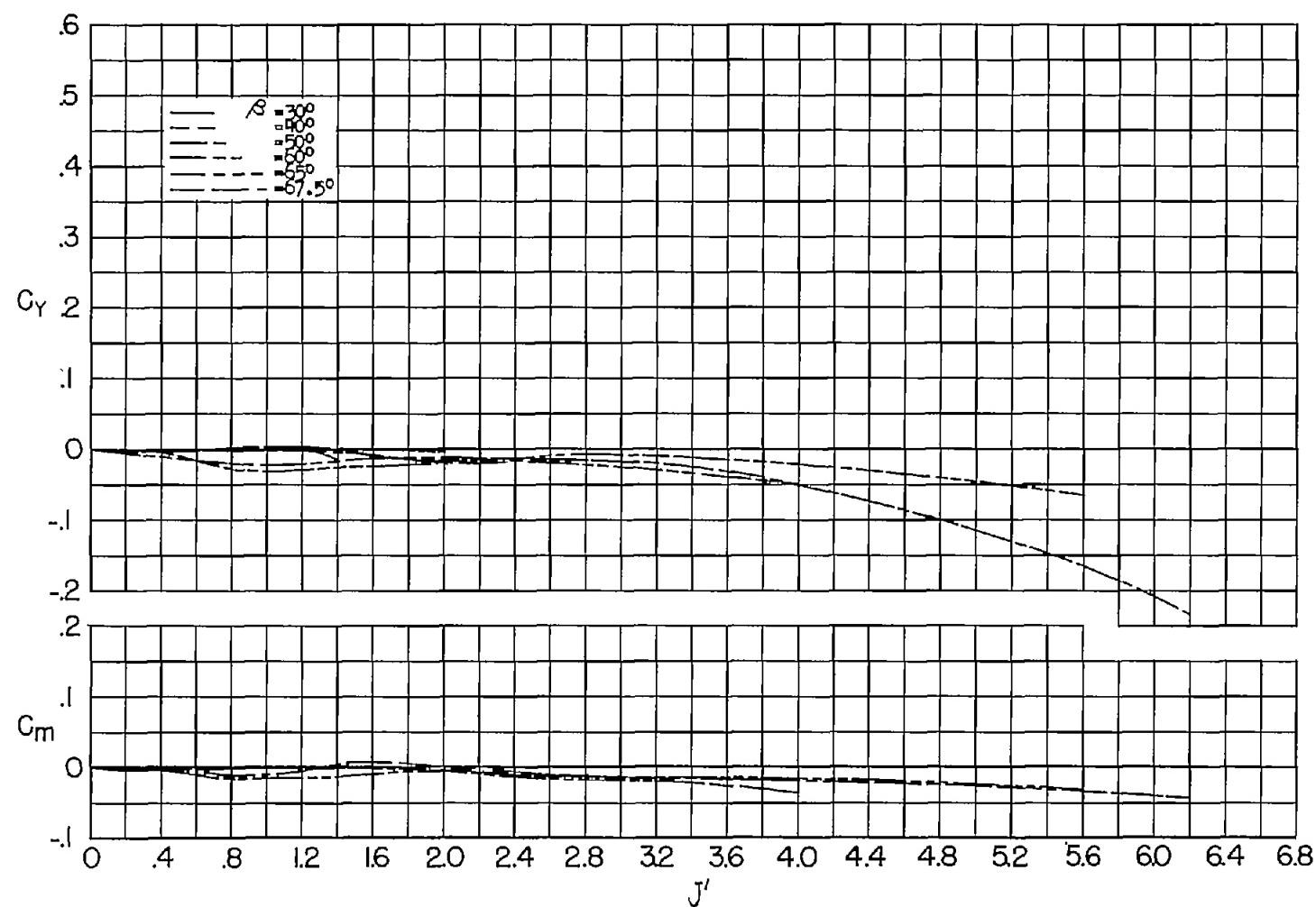
(e) C_Y and C_m against J'.

Figure 7.- Concluded.
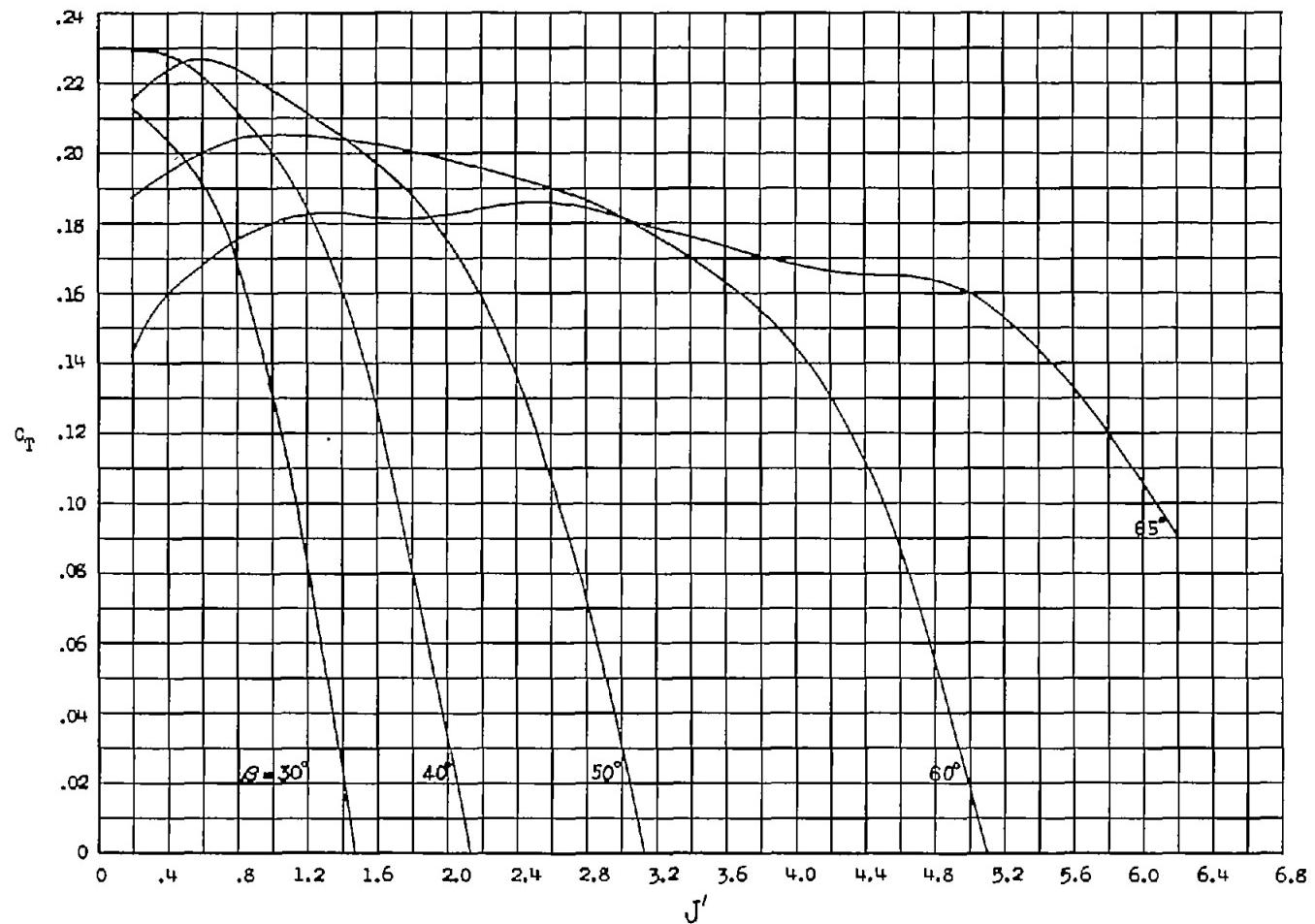
(a) C_T against J'.

Figure 8.- Variation of thrust, power, normal-force, and yawing- and pitching-moment coefficients with J'. $\alpha = 15°$.
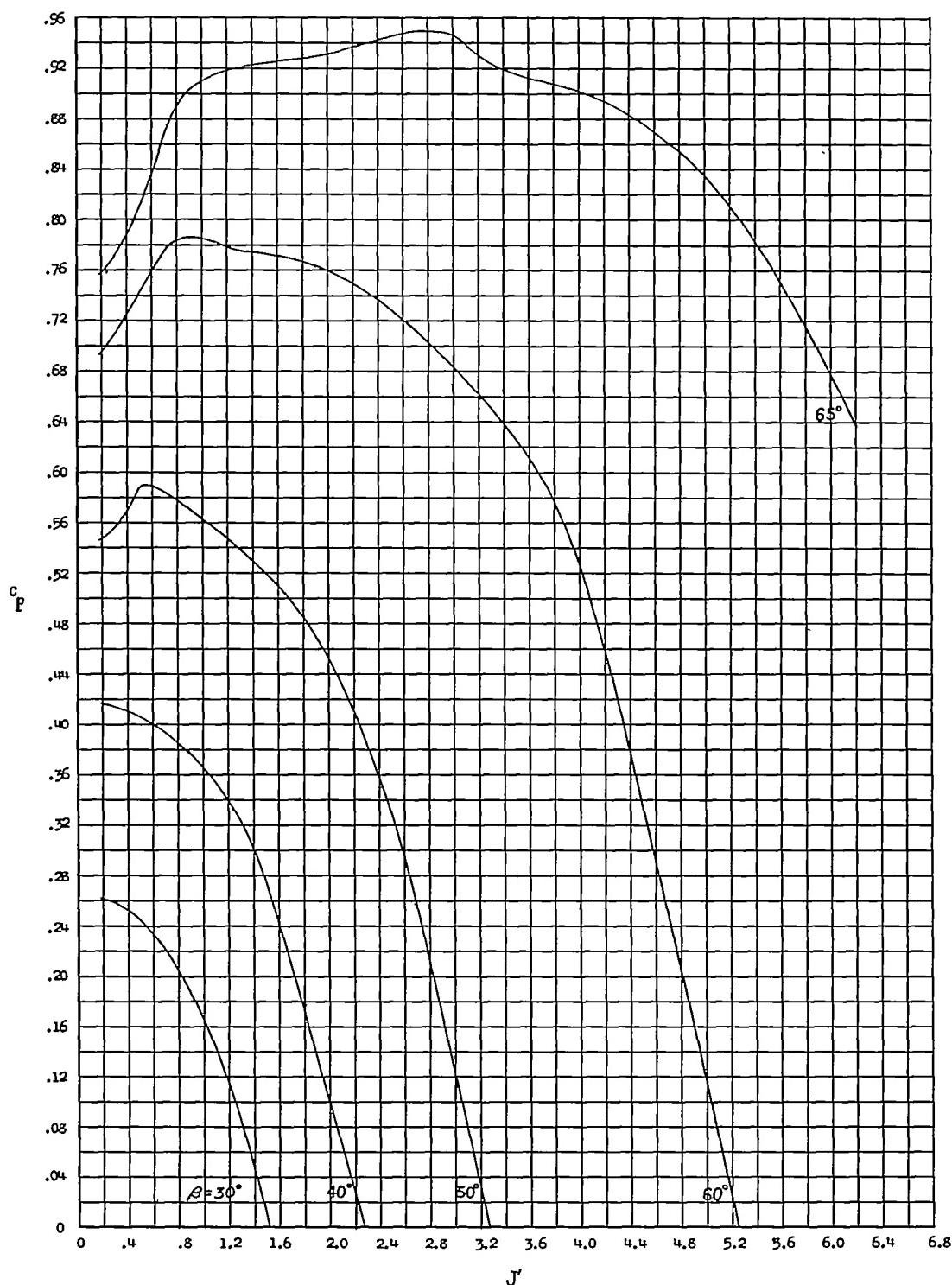
(b) Cp against J'.

Figure 8.- Continued.
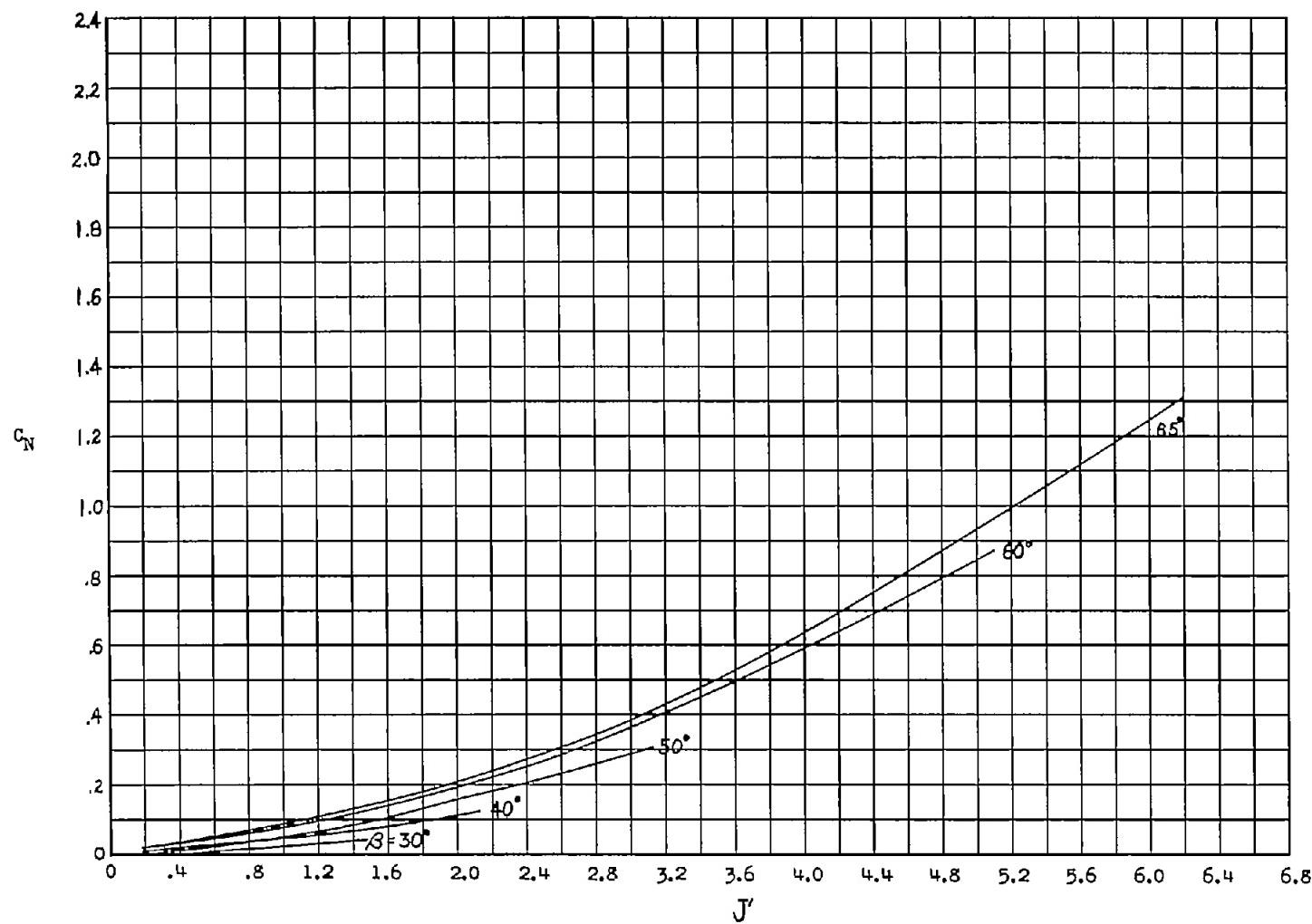
(c) C_N against J'.

Figure 8.- Continued.
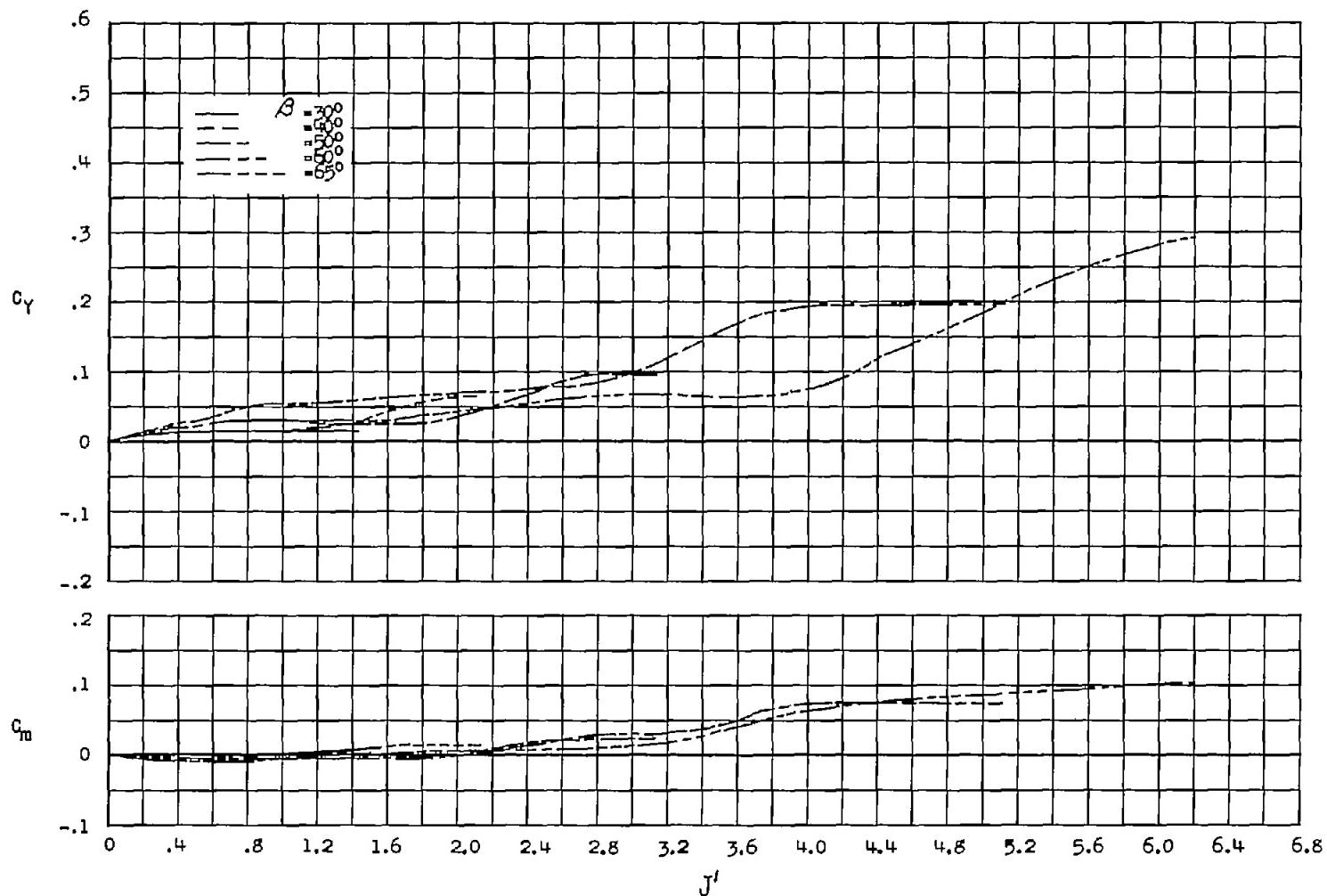
(d) C_Y and C_m against J'.

Figure 8.- Concluded.
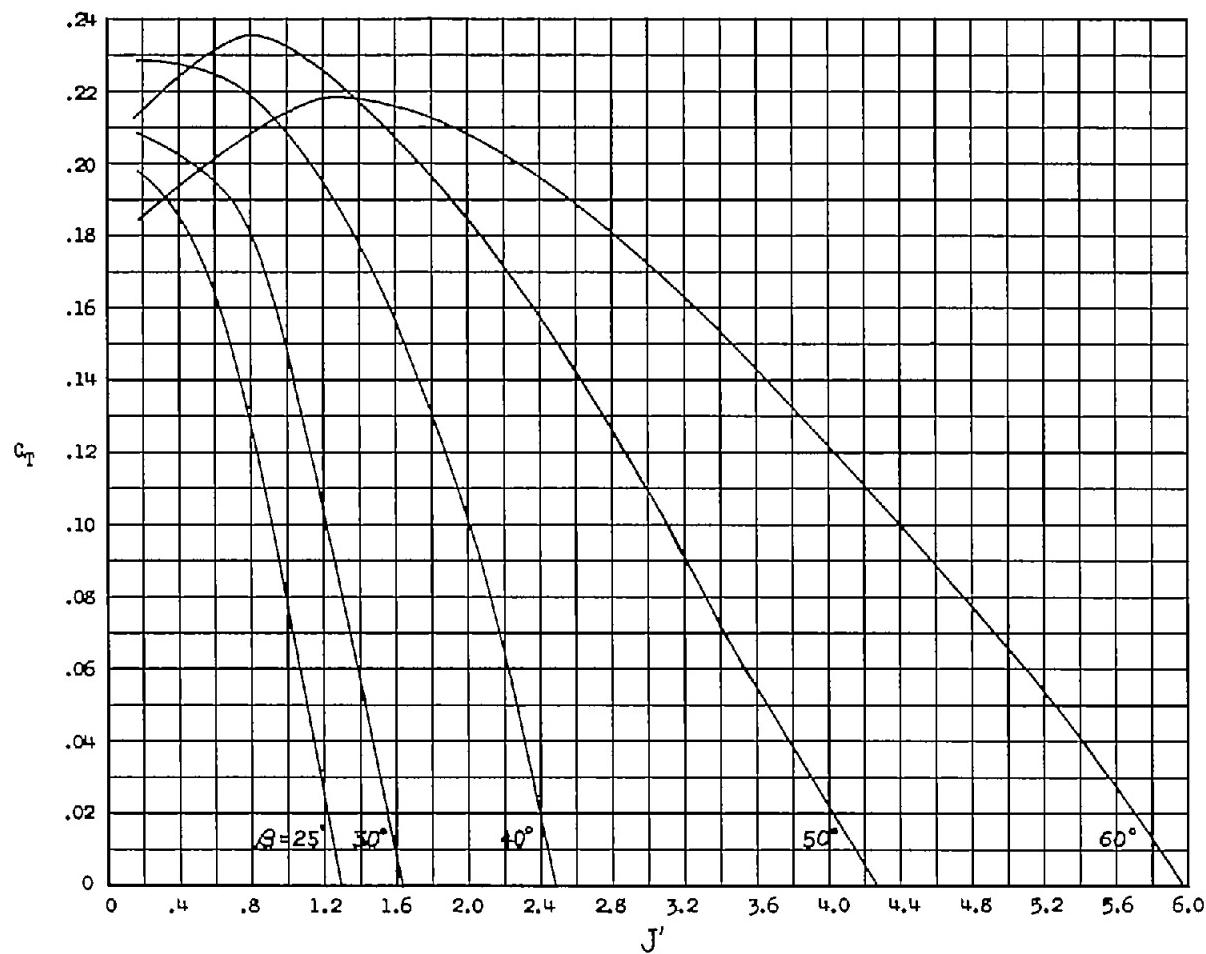
(a) C_T against J'.

Figure 9.- Variation of thrust, power, normal-force, yawing-, and pitching-moment coefficients with J'. $\alpha = 30°$.
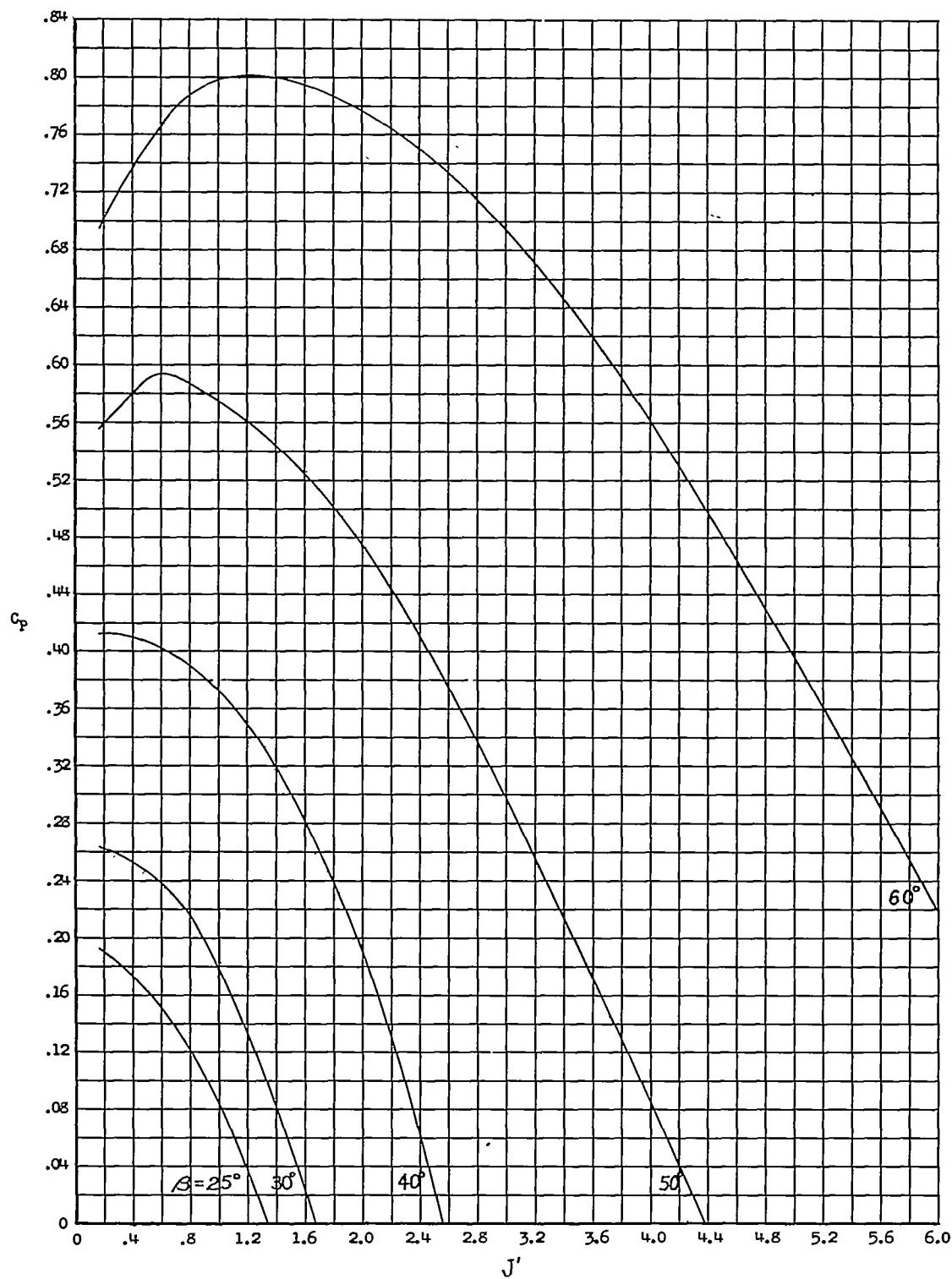
(b) C_P against J'.

Figure 9.- Continued.
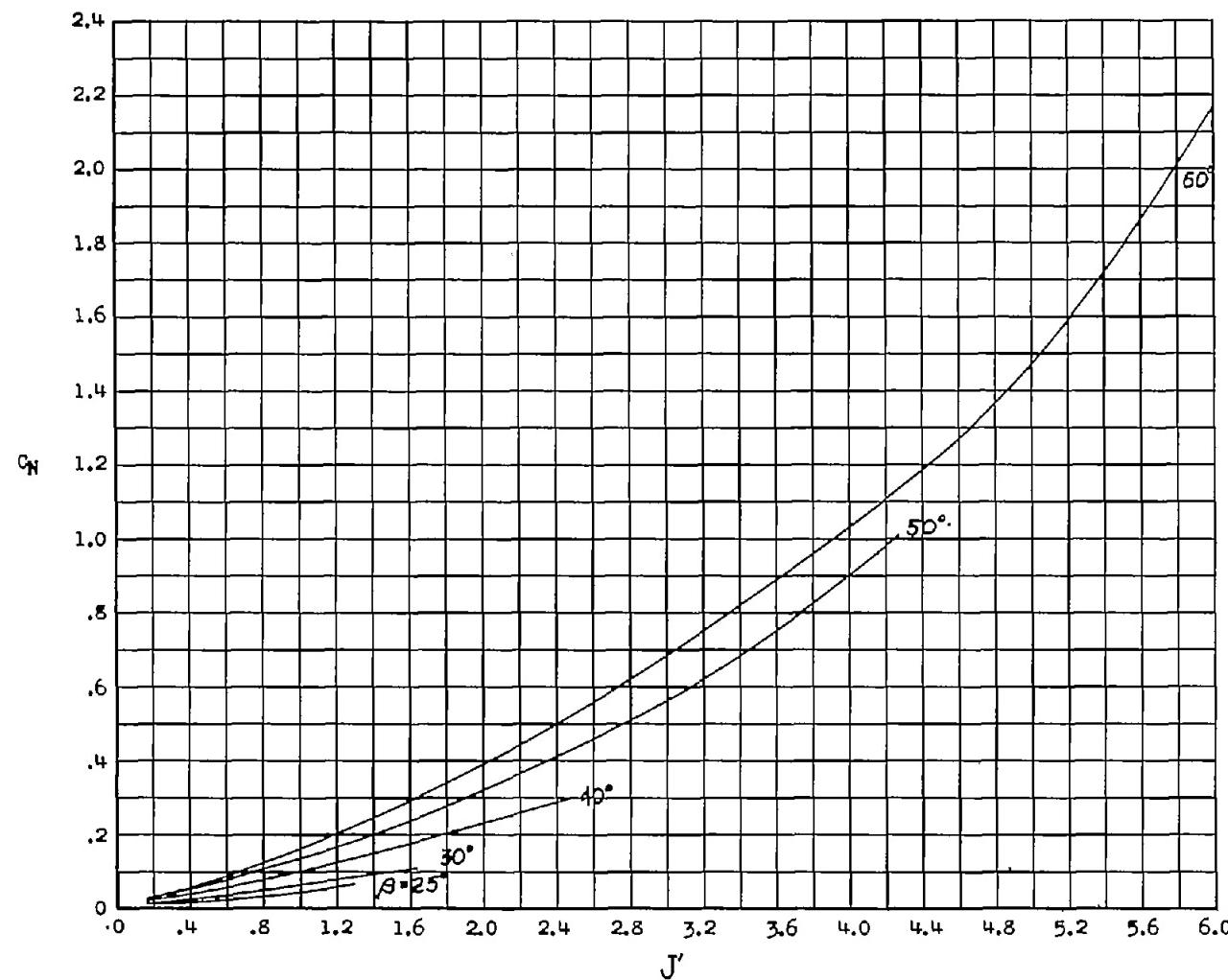
(c) C_N against J'.

Figure 9.- Continued.
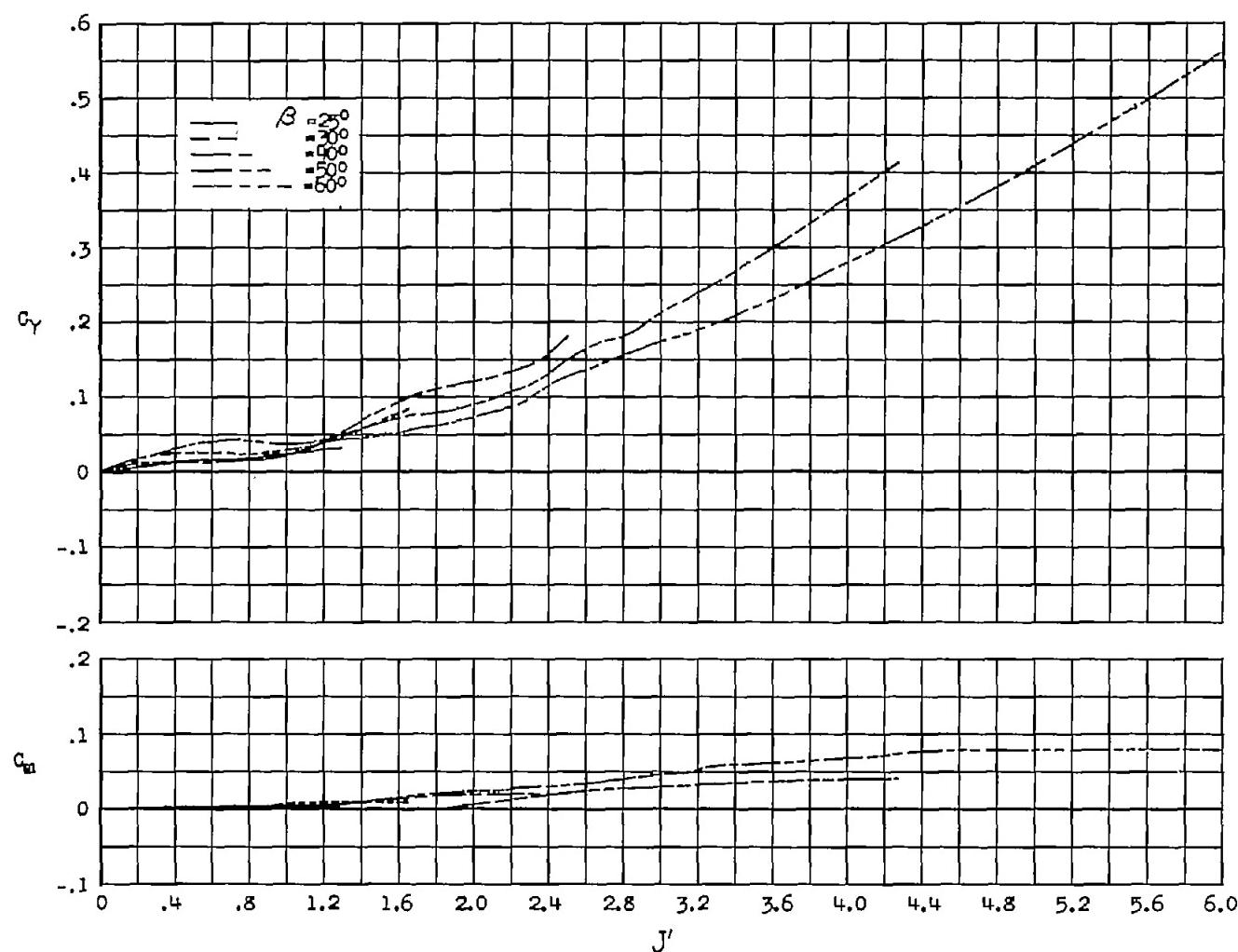
(d) C_Y and C_m against J'.

Figure 9.- Concluded.
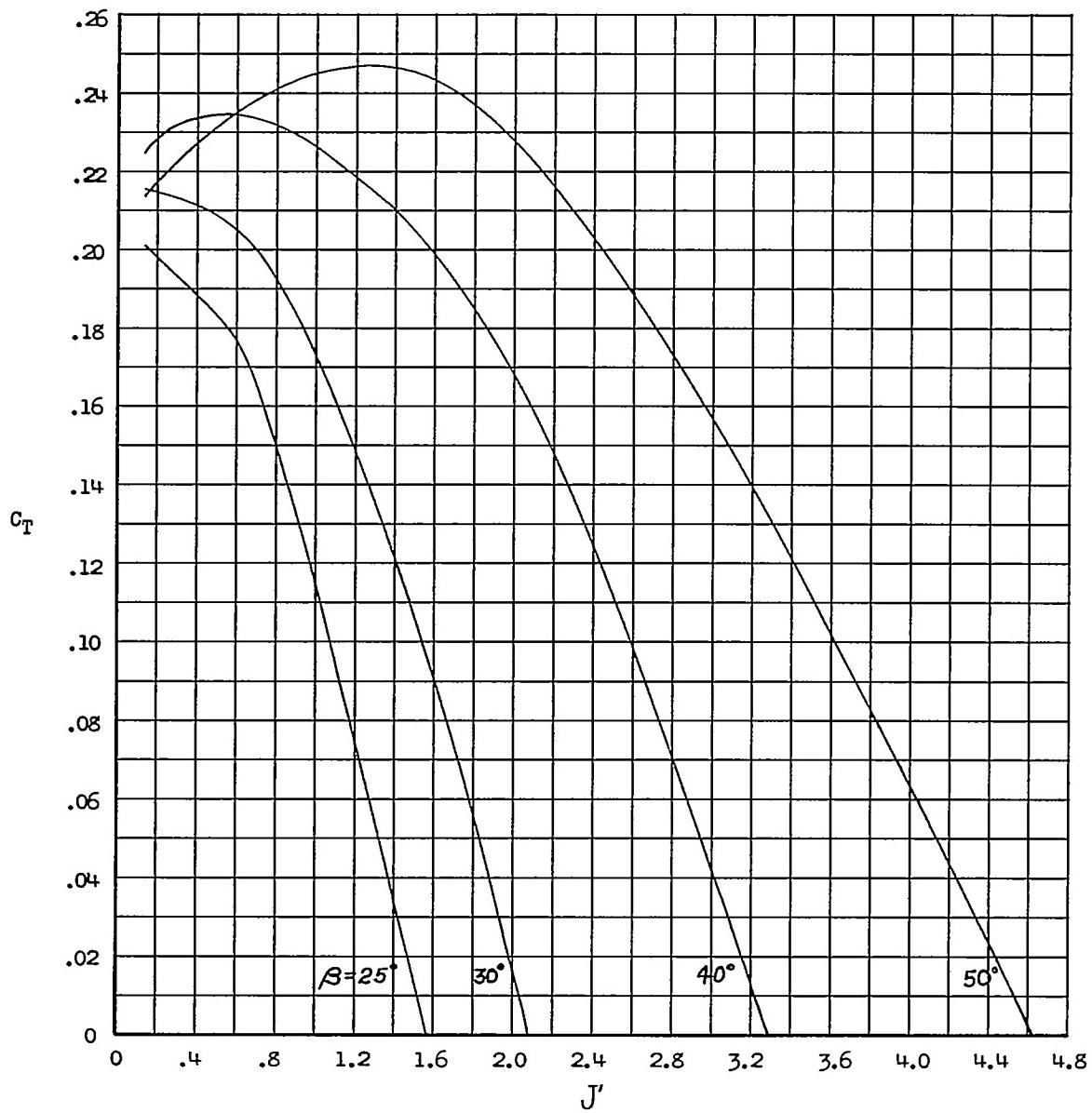
(a) C_T against J'.

Figure 10.- Variation of thrust, power, normal-force, yawing-, and pitching-
moment coefficients with J'. $\alpha = 45^\circ$.
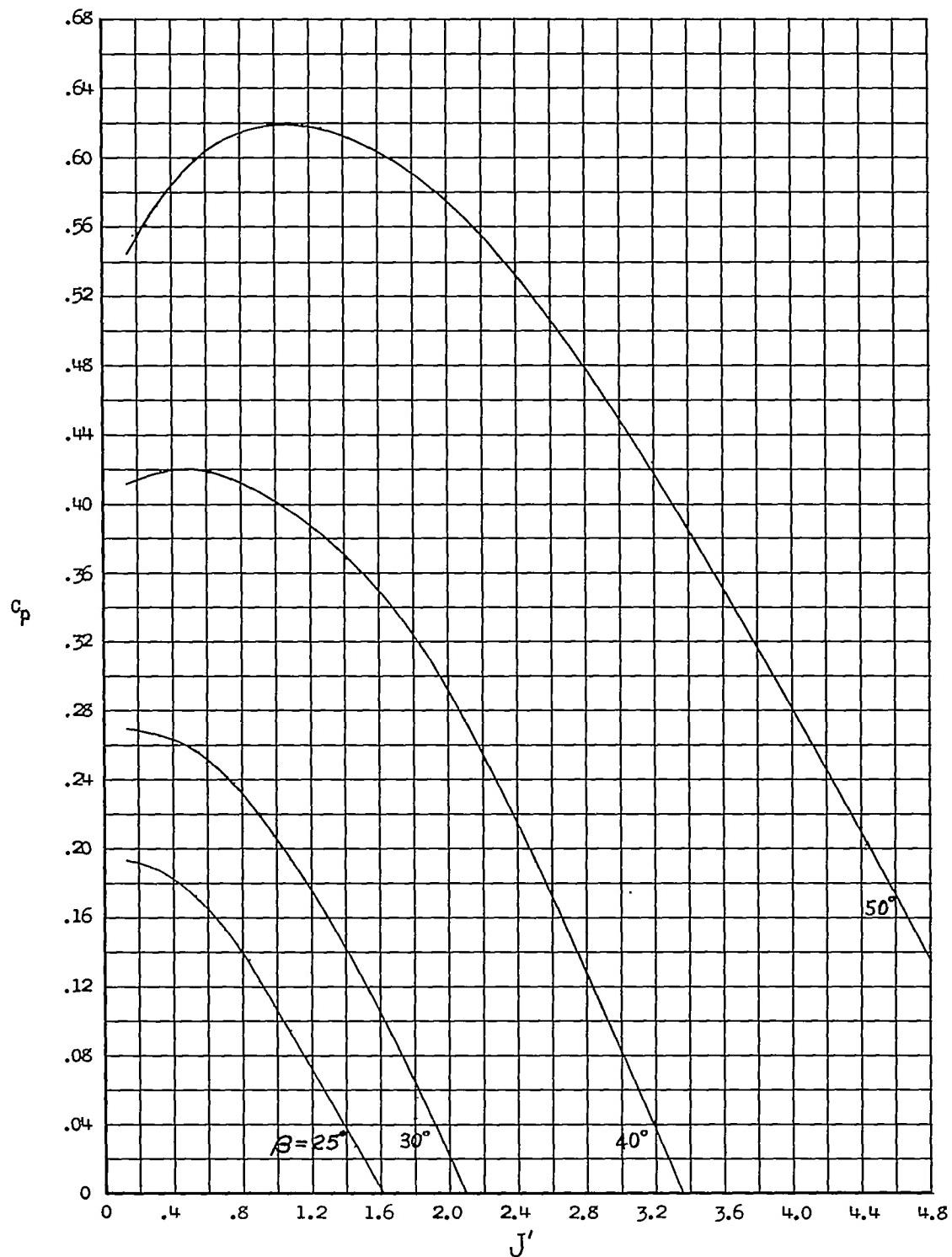
(b) C_P against J'.

Figure 10.- Continued.
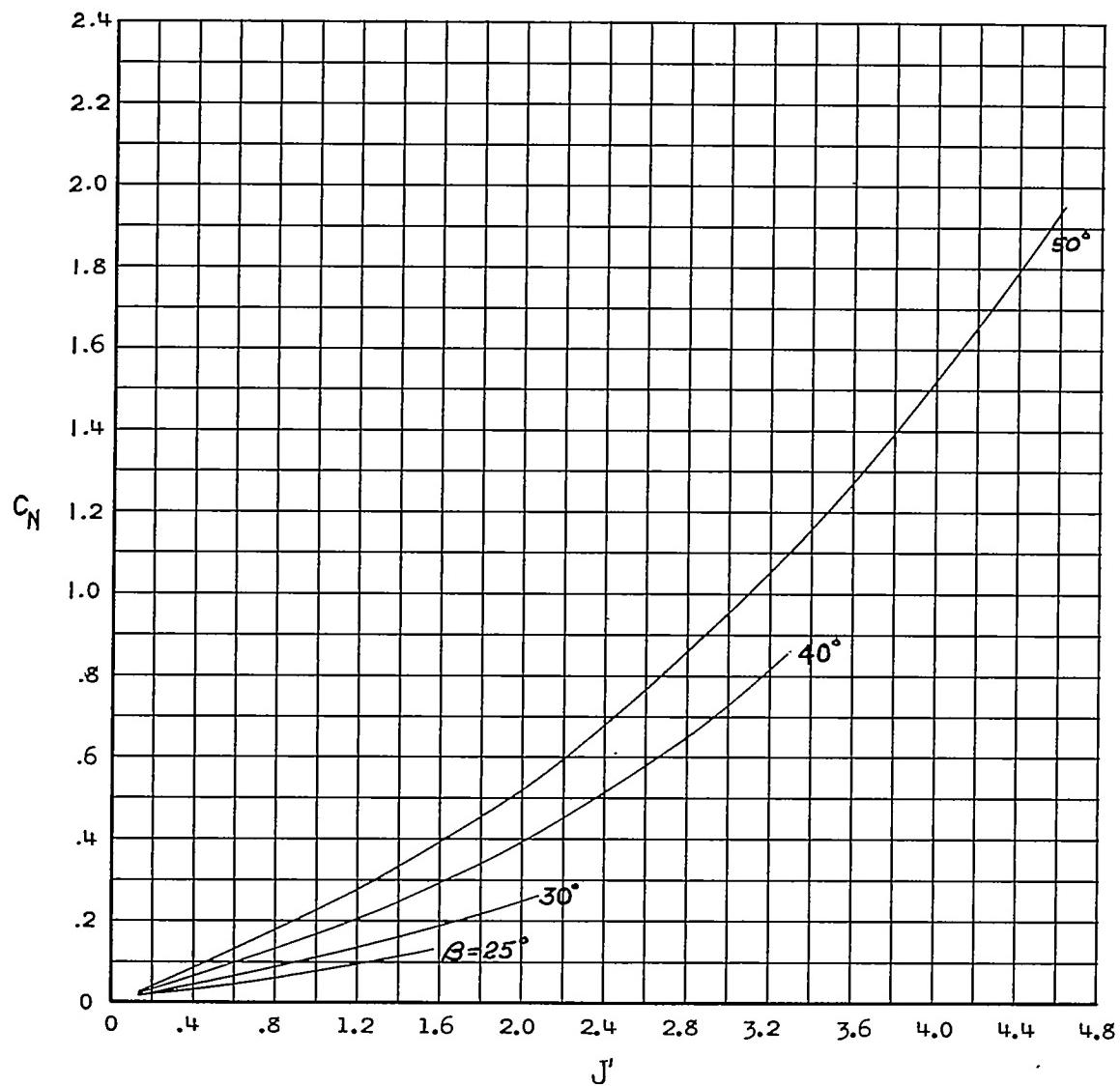
(c) C_N against J'.

Figure 10.- Continued.
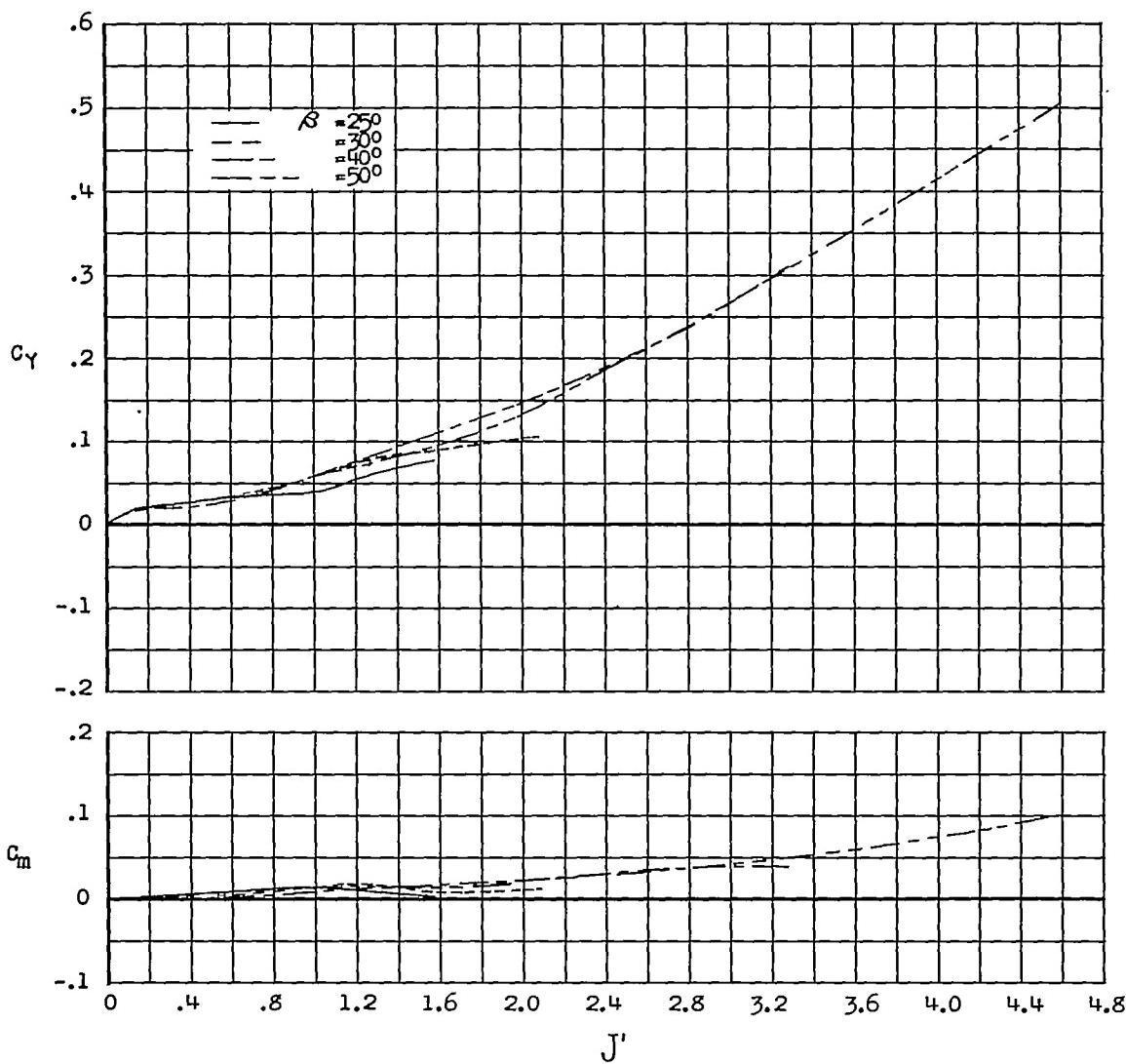
(d) C_Y and C_m against J'.

Figure 10.- Concluded.
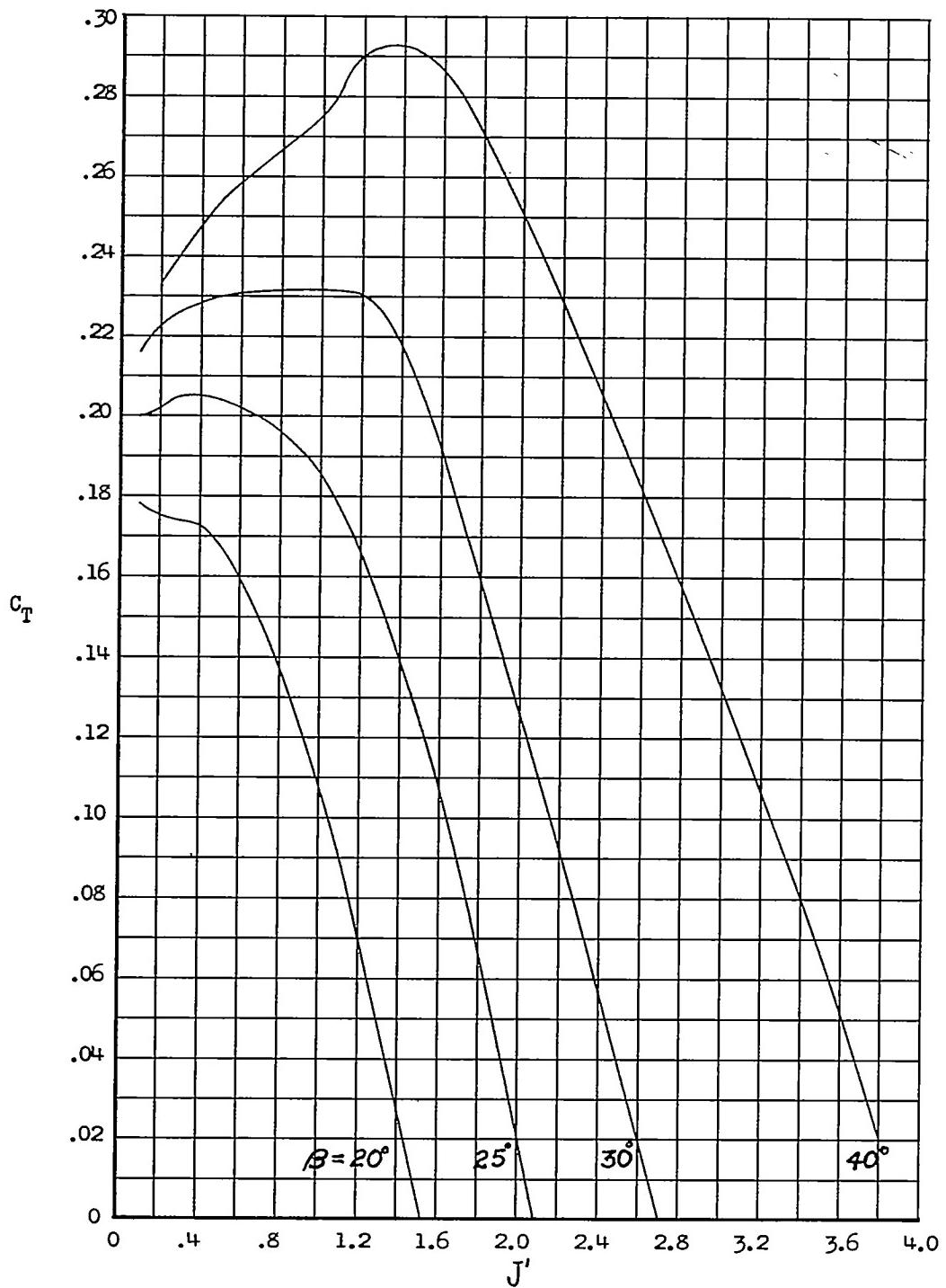
(a) C_T against J'.

Figure 11.- Variation of thrust, power, normal-force, yawing-, and pitching-
moment coefficients with J'. $\alpha = 60°$.
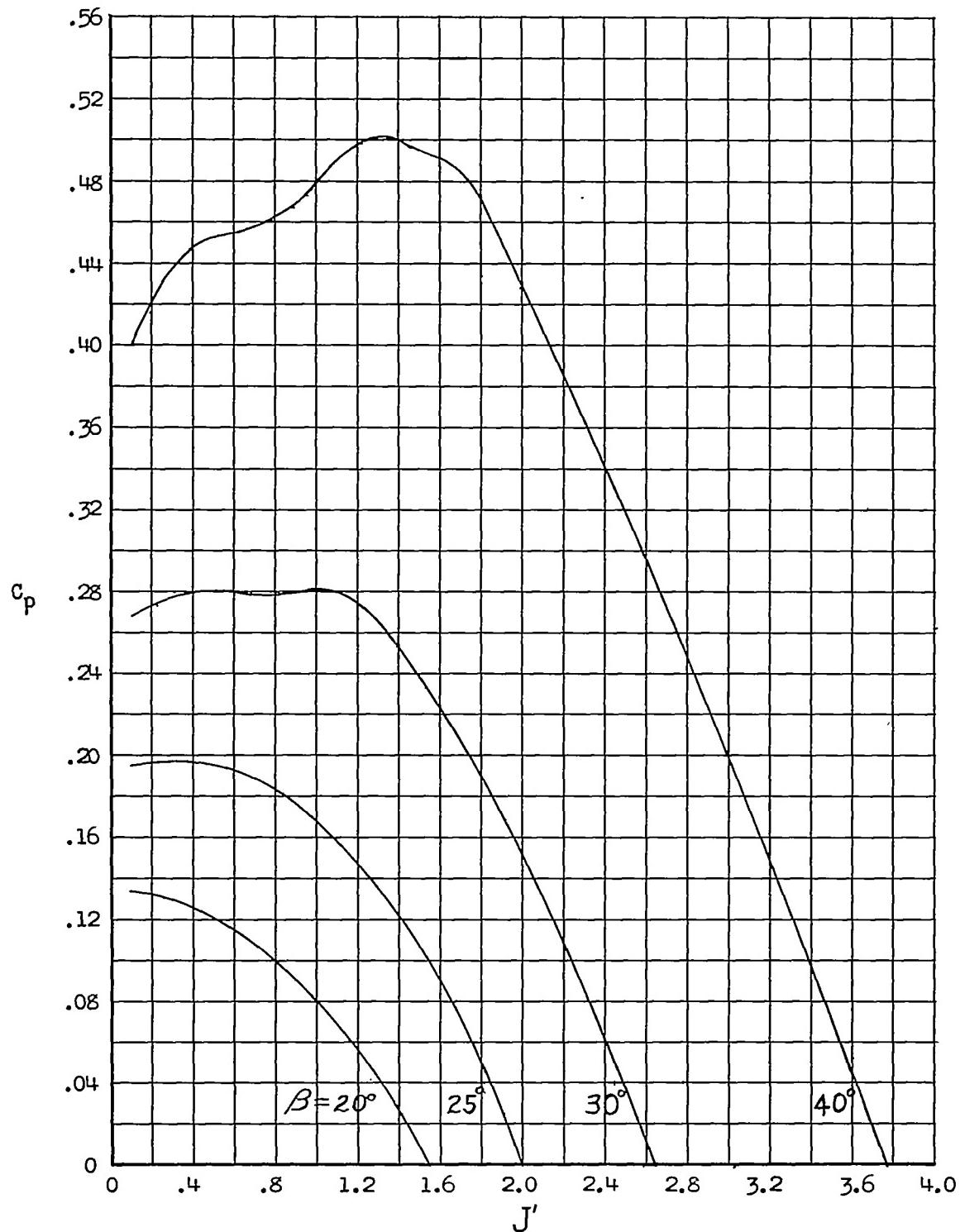
(b) C_P against J'.

Figure 11.- Continued.
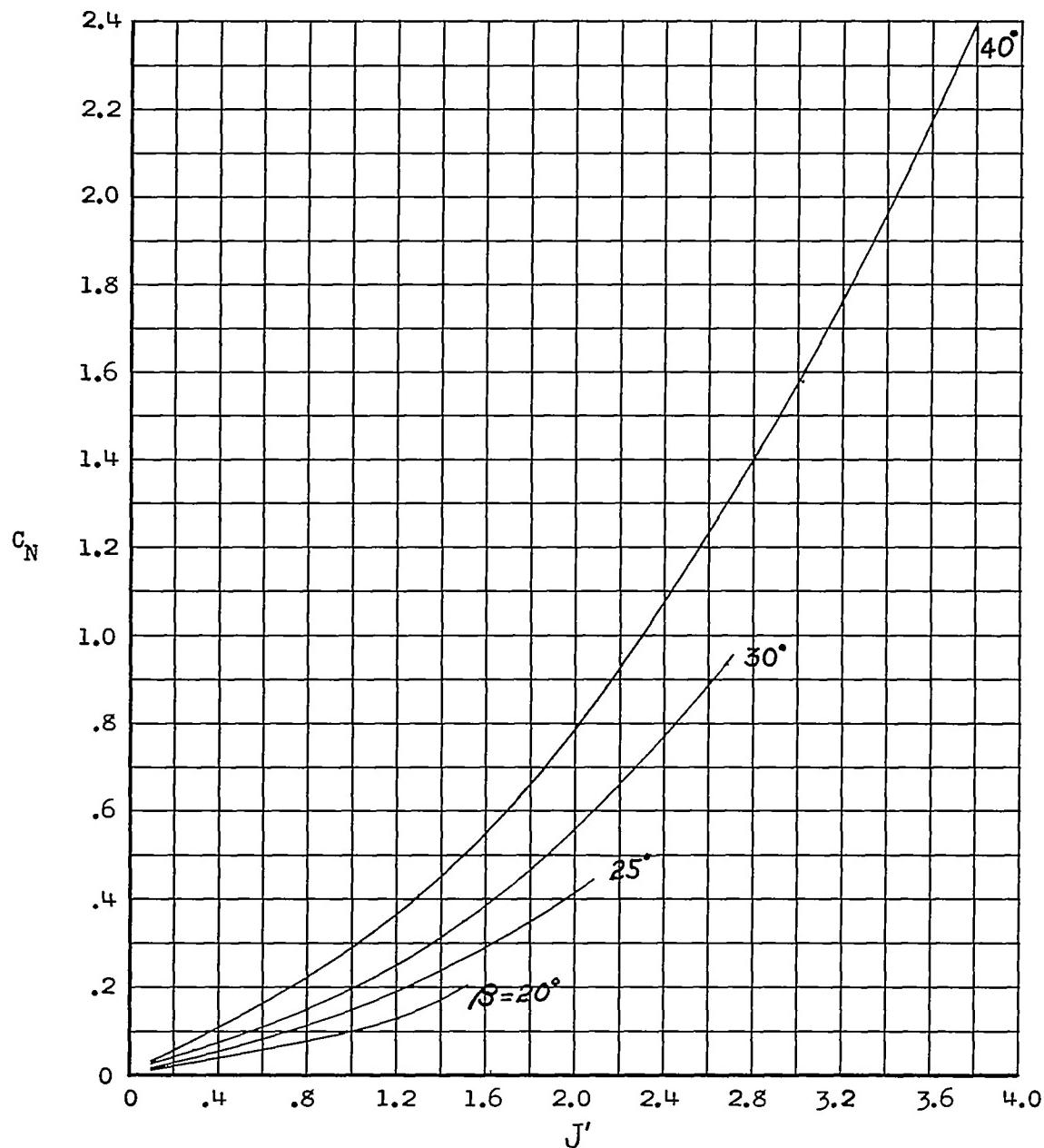
(c) C_N against J'.

Figure 11.- Continued.
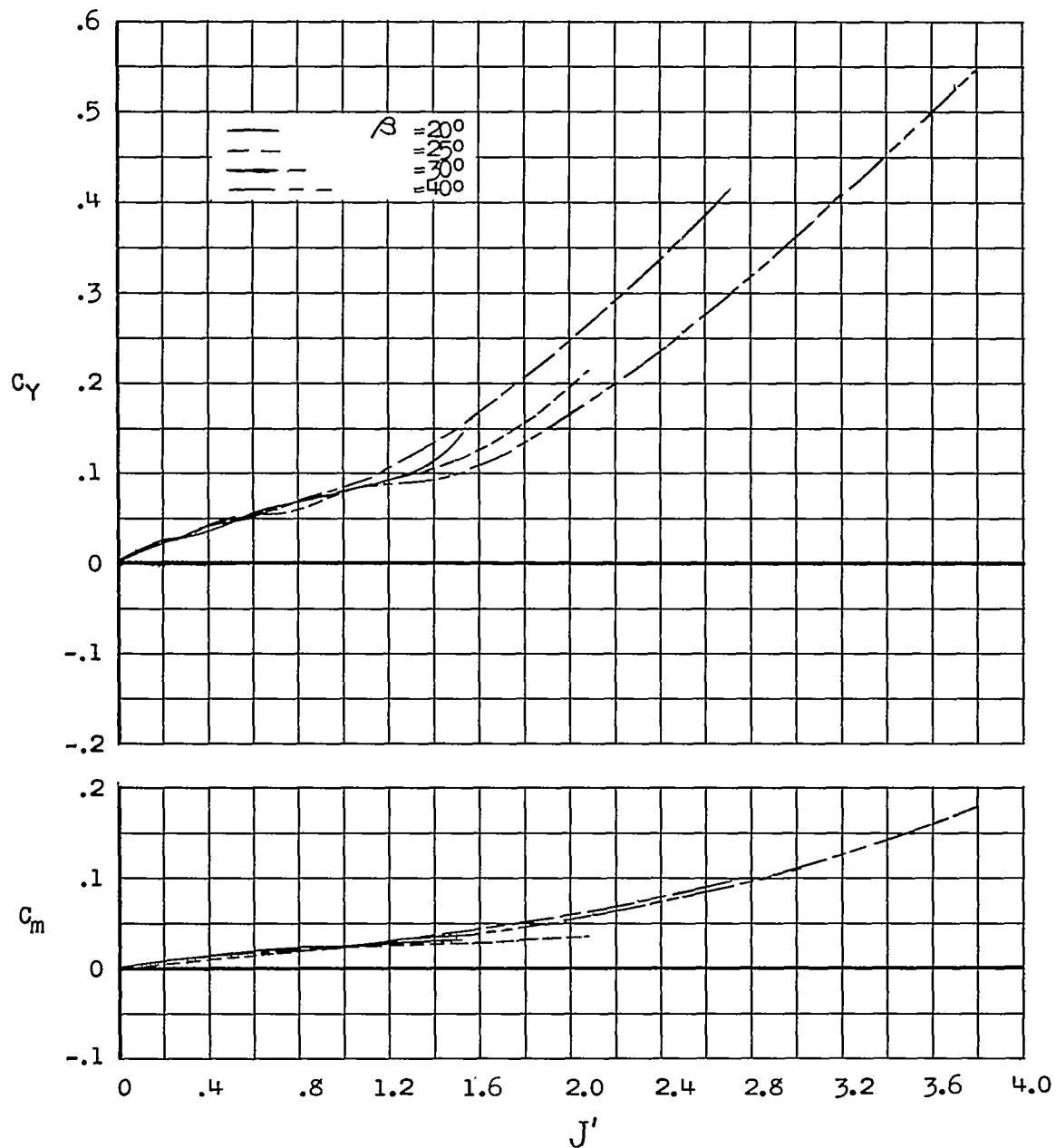
(d) C_Y and C_m against J'.

Figure 11.- Concluded.
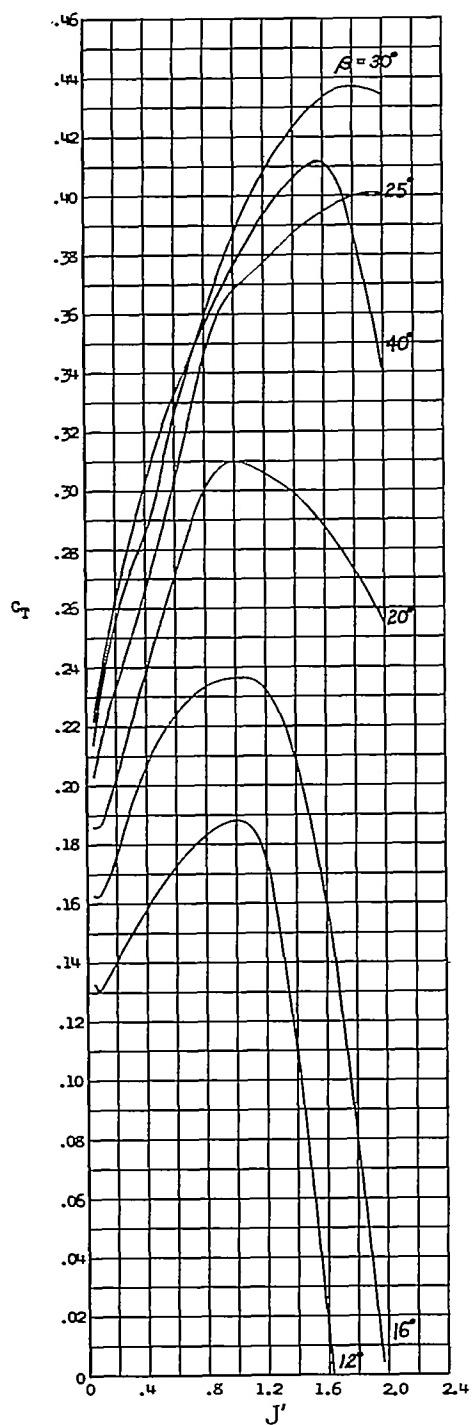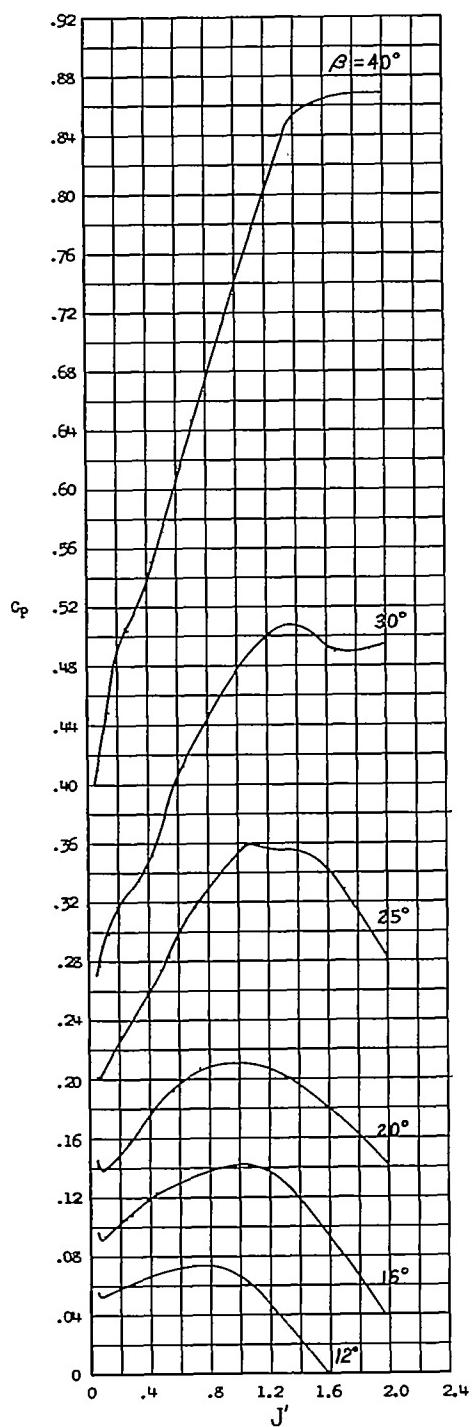
(a) C_T against J'.   (b) C_P against J'.

Figure 12.- Variation of thrust, power, normal-force, yawing-, and pitching-
moment coefficients with J'. $\alpha = 75^\circ$.
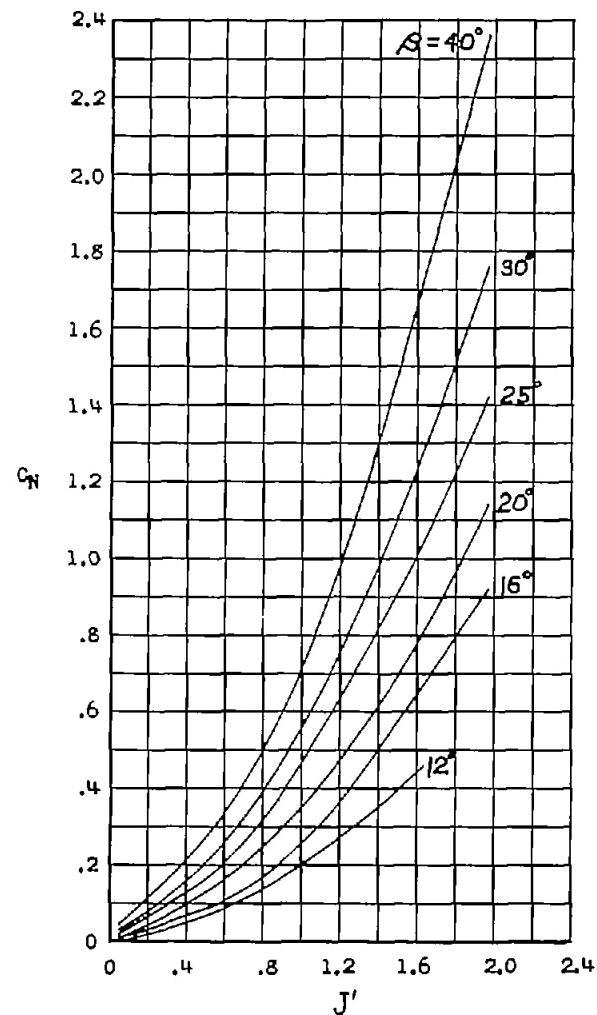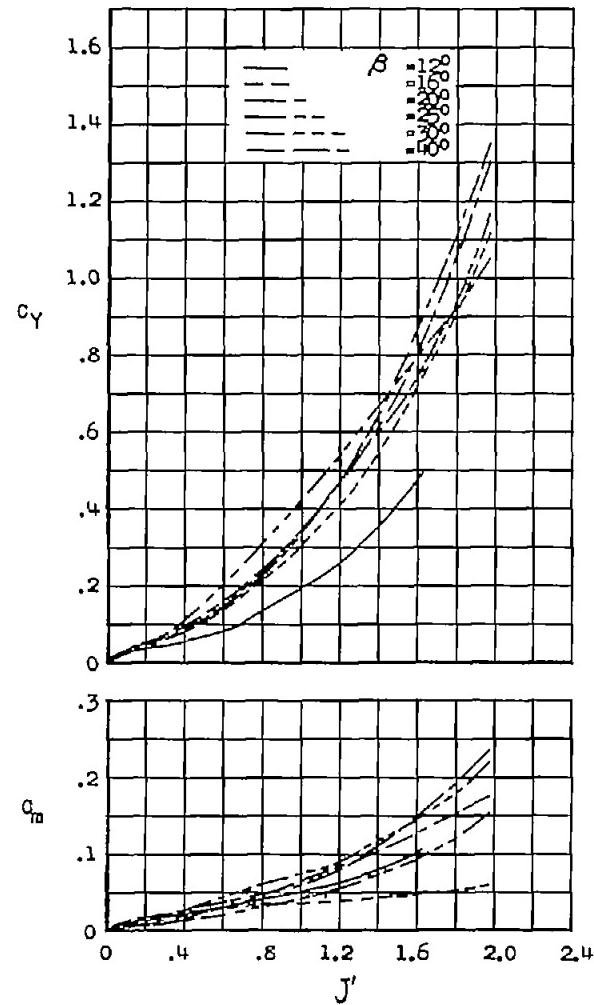
(c) C_N against J'.   (d) C_Y and C_m against J'.

Figure 12.- Concluded.
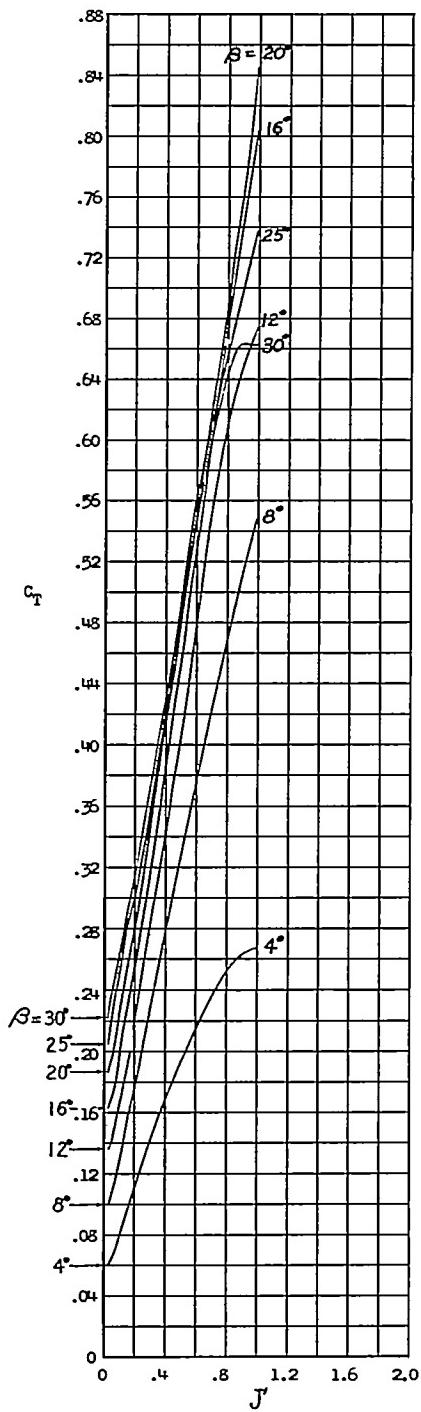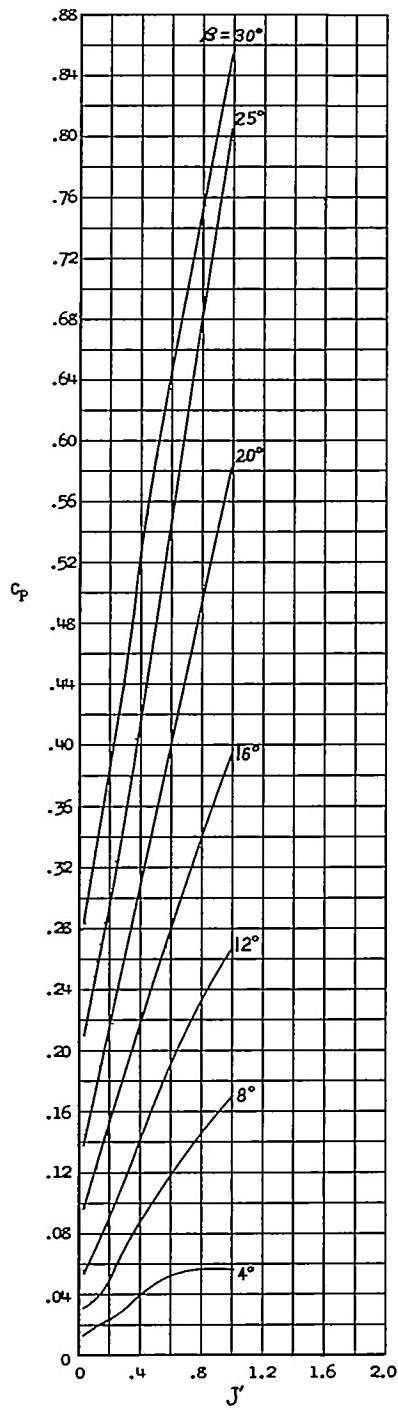
(a) C_T against J'.   (b) C_P against J'.

Figure 13.- Variation of thrust, power, normal-force, yawing-, and pitching-
moment coefficients with J'. $\alpha = 82.5°$.
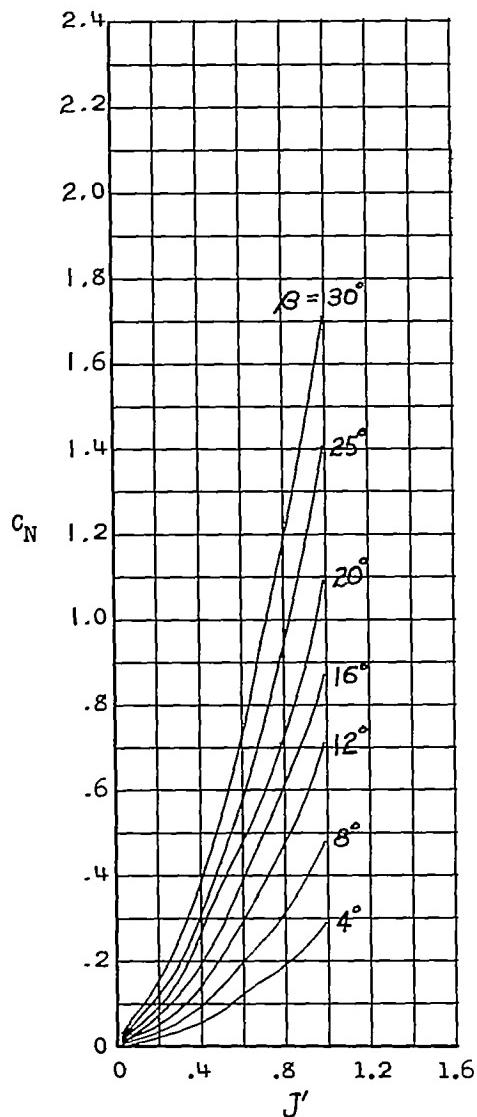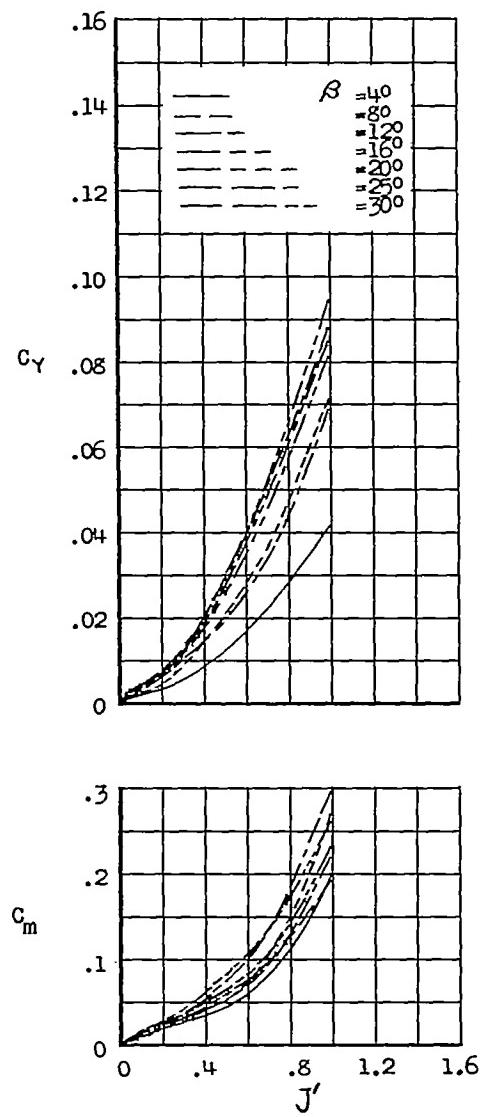
(c) C_N against J'.   (d) C_Y and C_m against J'.

Figure 13.- Concluded.
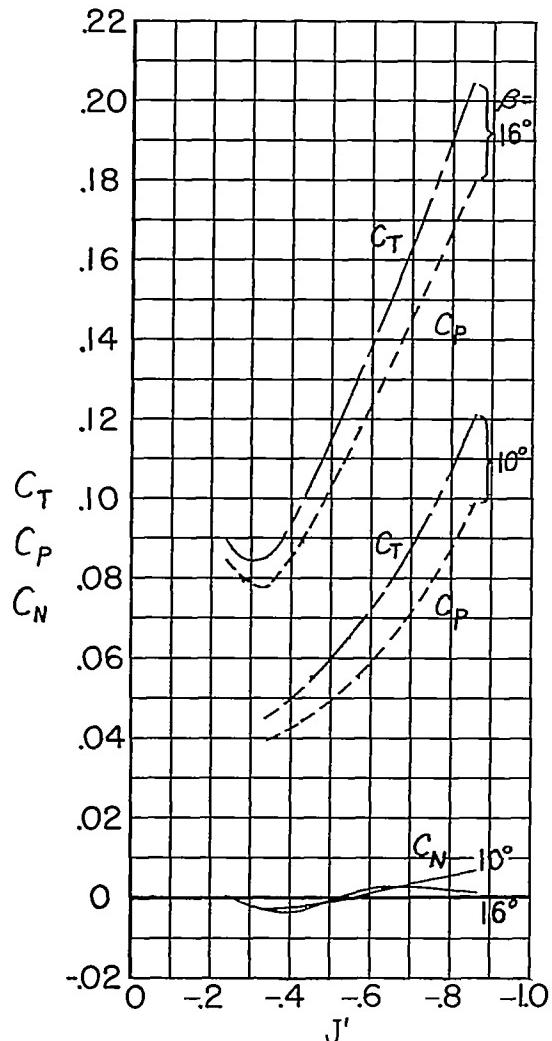
(a) C_T, C_P, and C_N against J'.   (b) C_T, C_P, and C_N against J'.
$\alpha = 165°$. $\alpha = 180°$.

Figure 14.- Aerodynamic characteristics of propeller for angles of attack
of 165° and 180°.
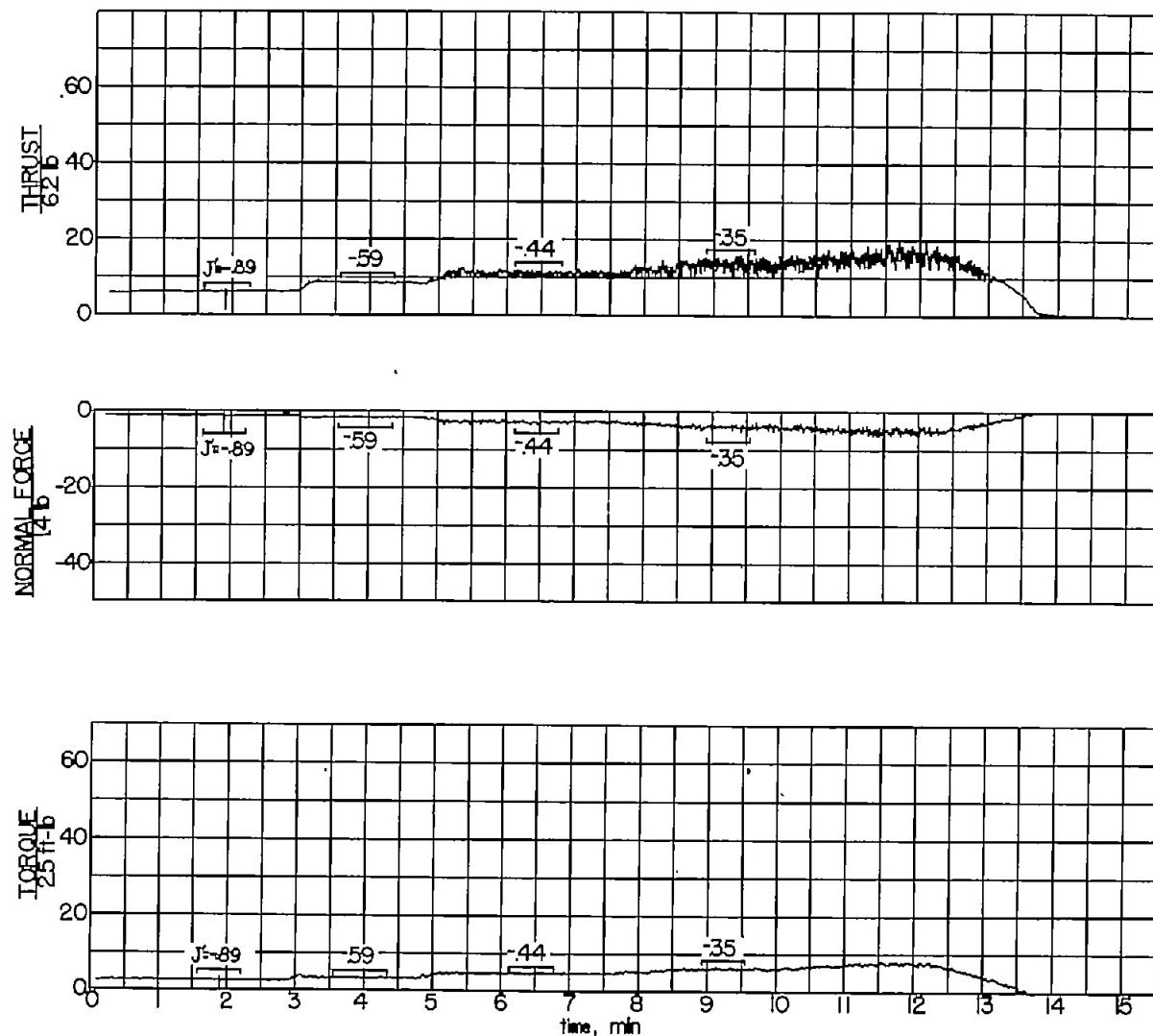
Figure 15.- Time history of thrust, normal force, and torque for several values of J'. $\alpha = 165°$; $\beta = 10°$.
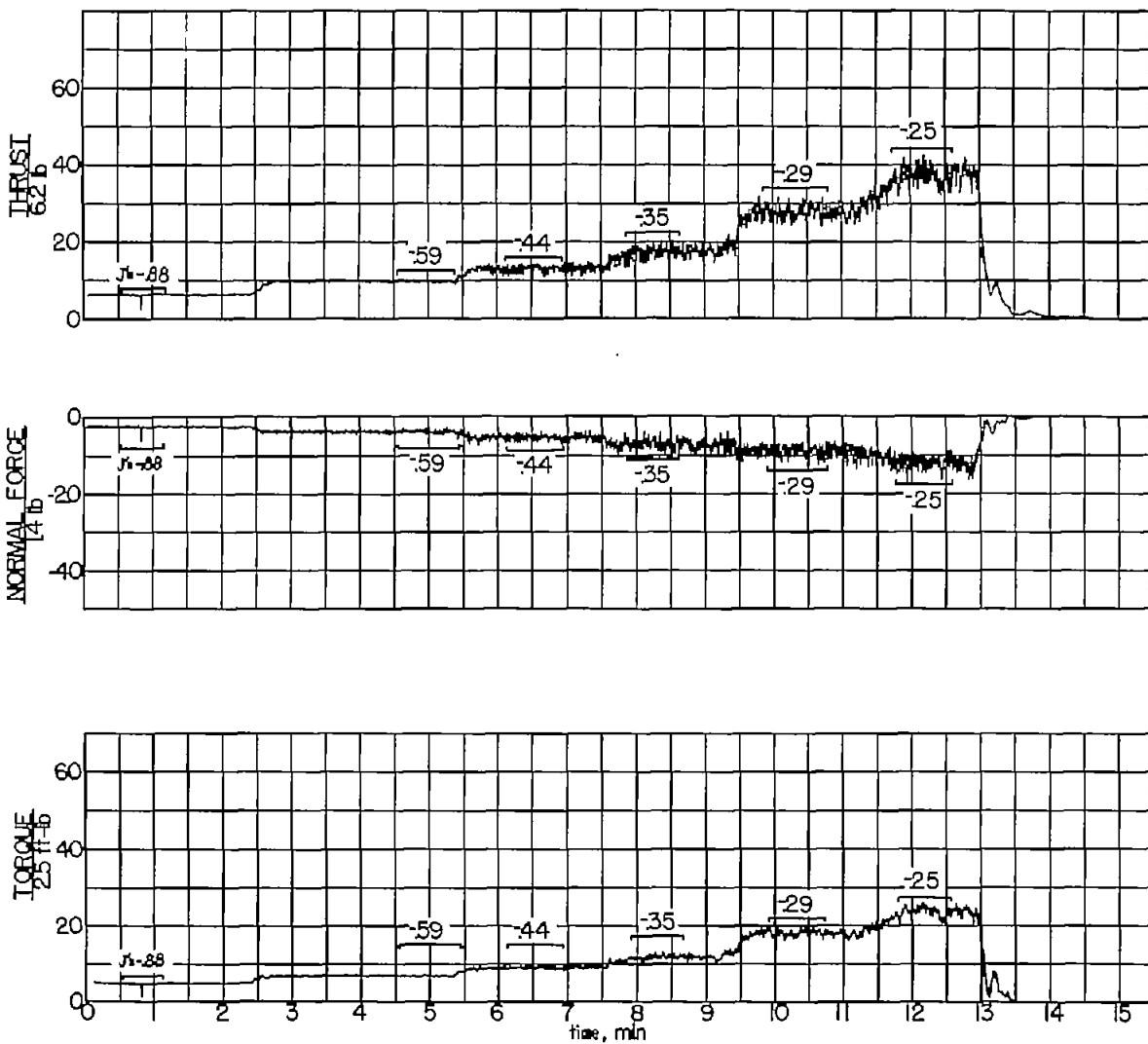
Figure 16.- Time history of thrust, normal force, and torque for several values of J'. α = 165°; β = 16°.
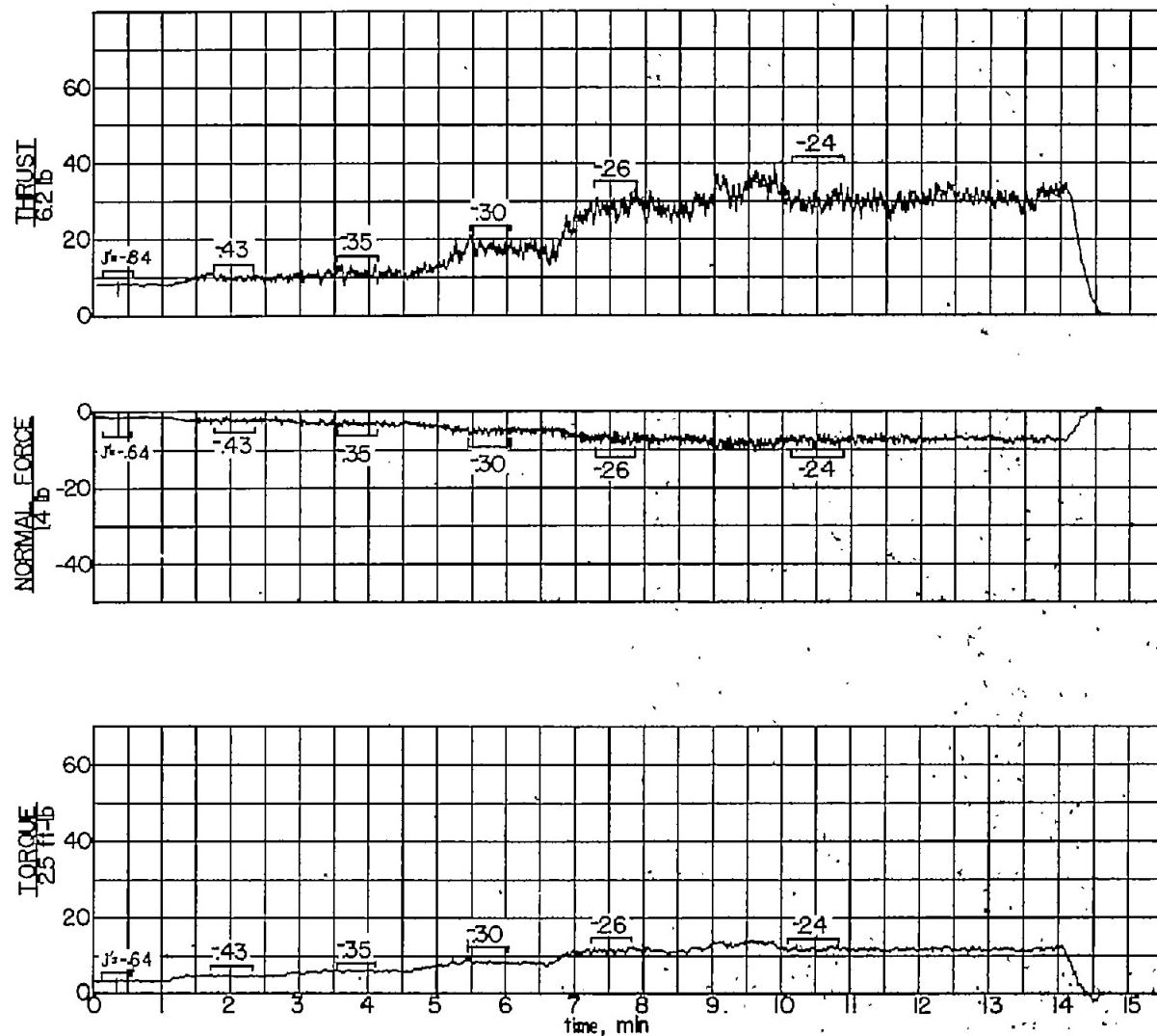
Figure 17.- Time history of thrust, normal force, and torque for several values of J'. $\alpha = 180^\circ$; $\beta = 10^\circ$.
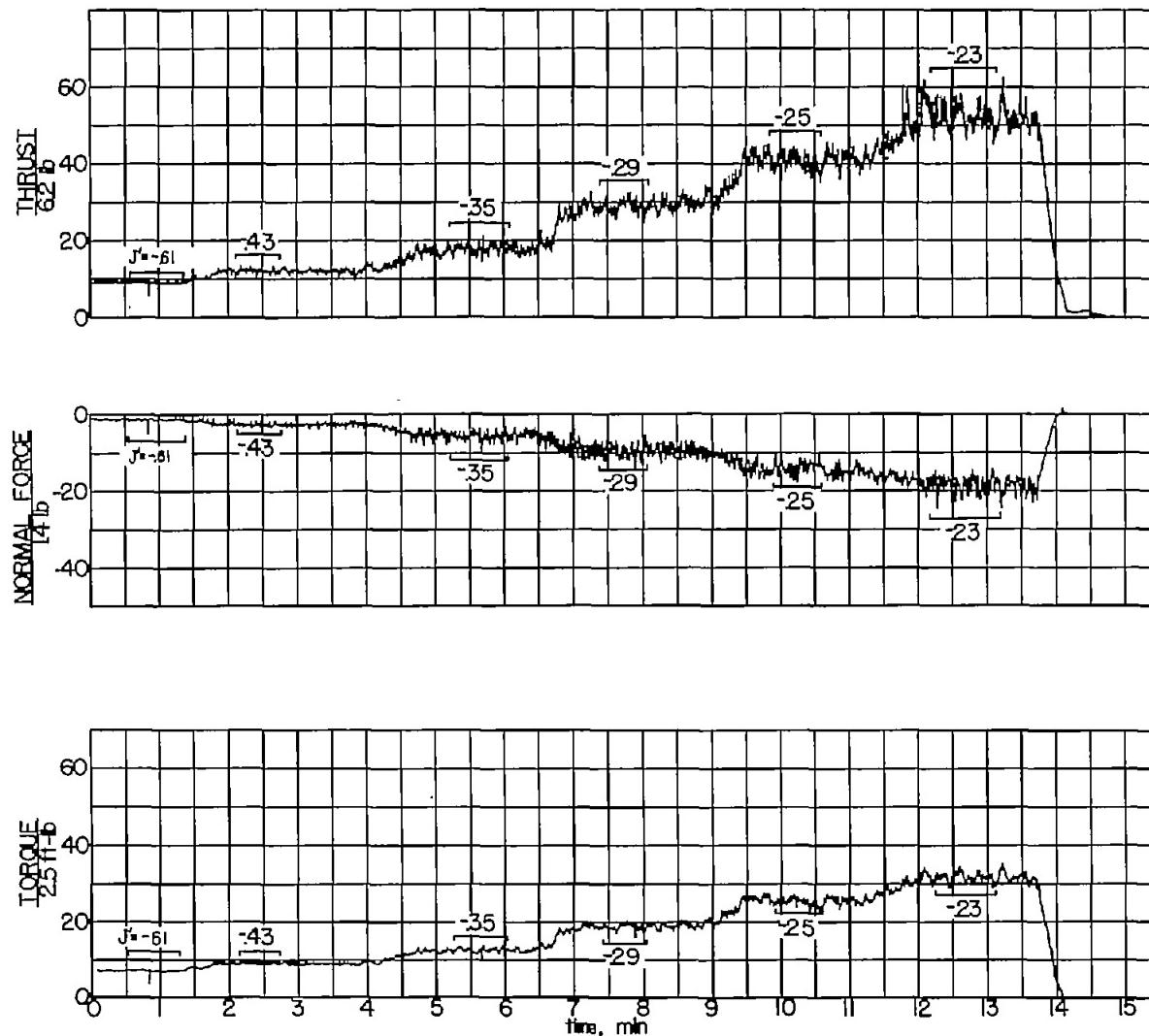
Figure 18.- Time history of thrust, normal force, and torque for several
values of J_{α}'. $\alpha = 180°$; $\beta = 16°$.
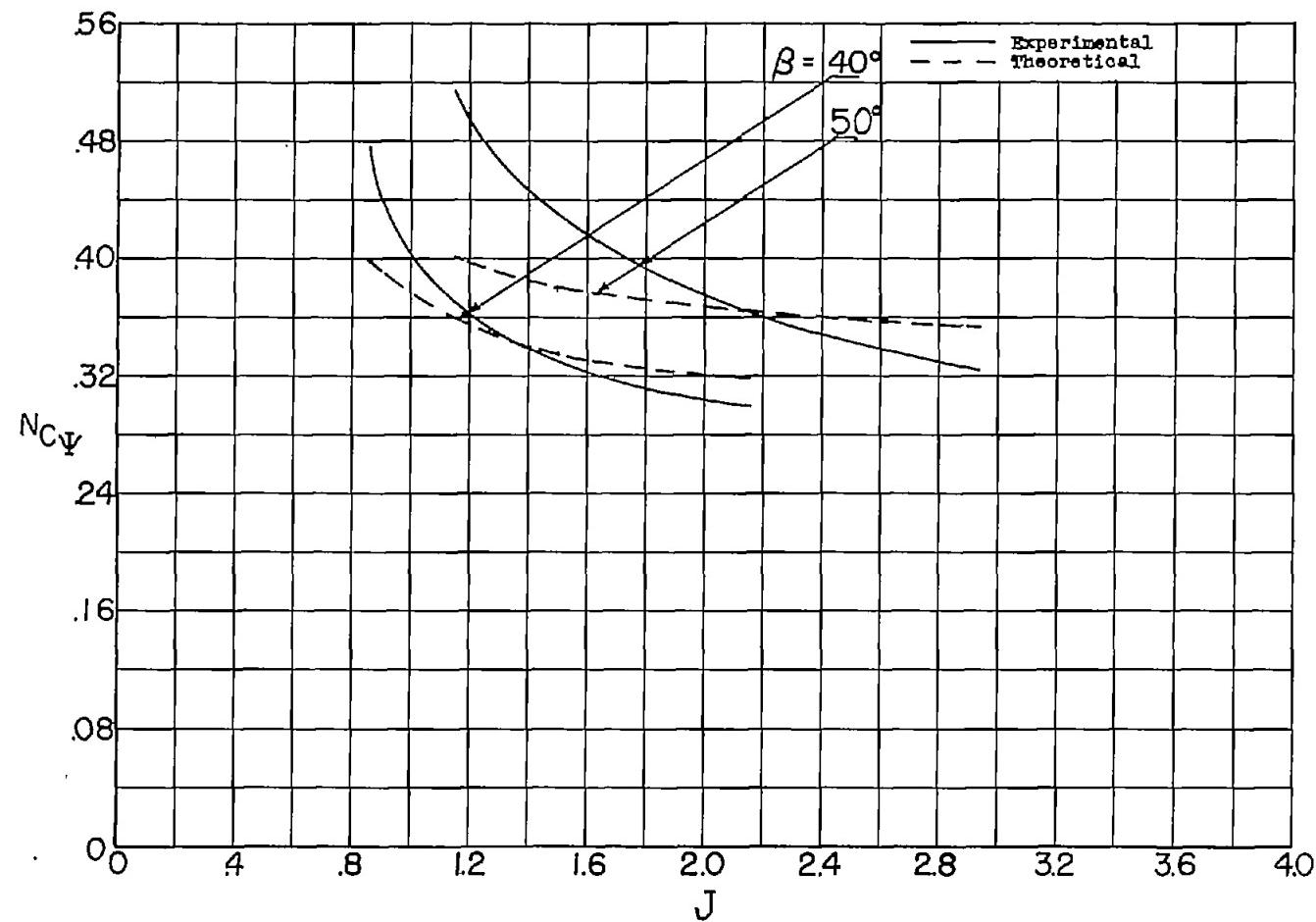
(a) $\alpha = 0°$.

Figure 19.- Comparison of theoretically and experimentally determined
values of rate of change of propeller normal-force coefficient with
angle of attack.
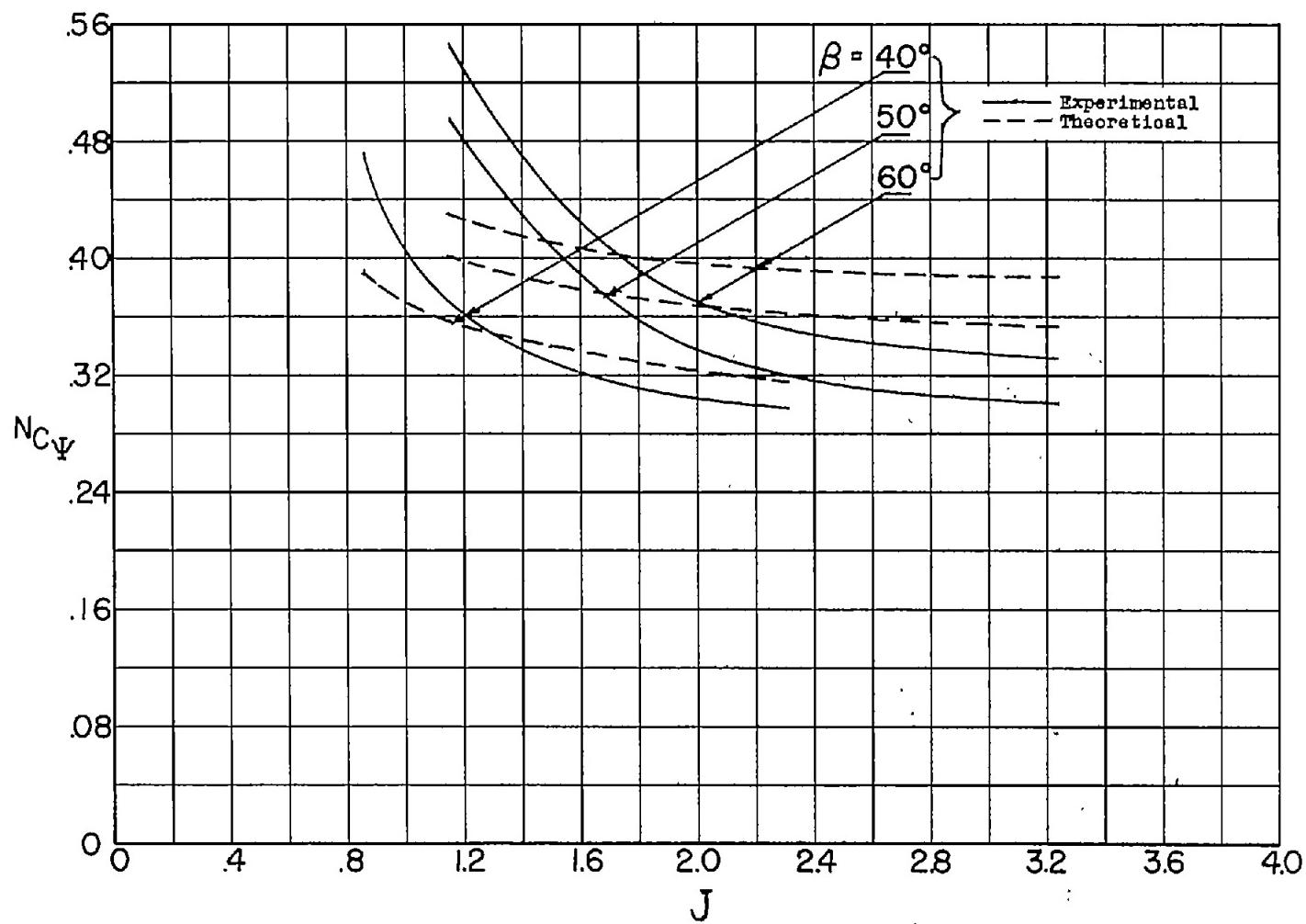
(b) $\alpha = 15°$.

Figure 19.- Continued.
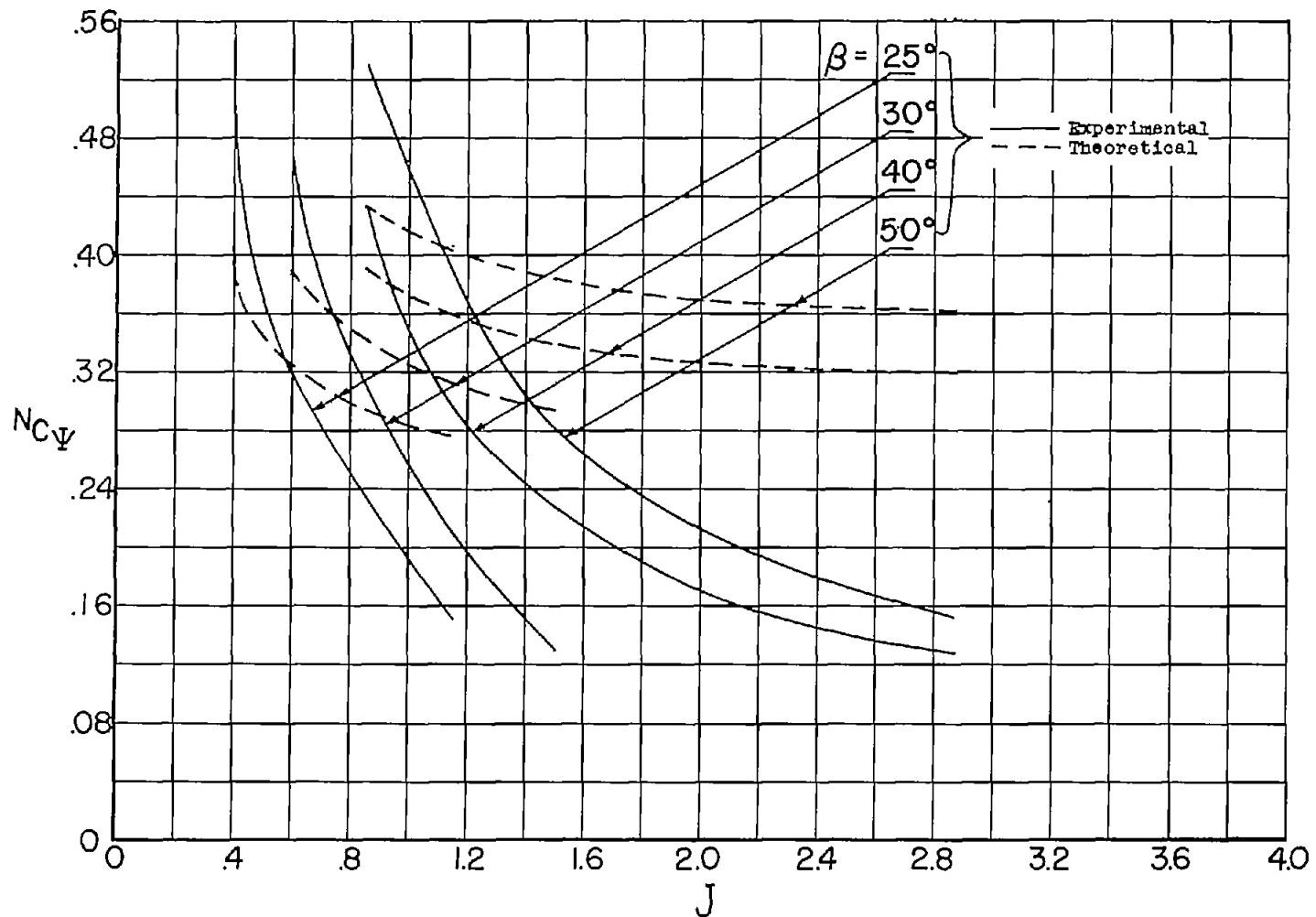
(c) $\alpha = 30^\circ$.

Figure 19.- Continued.
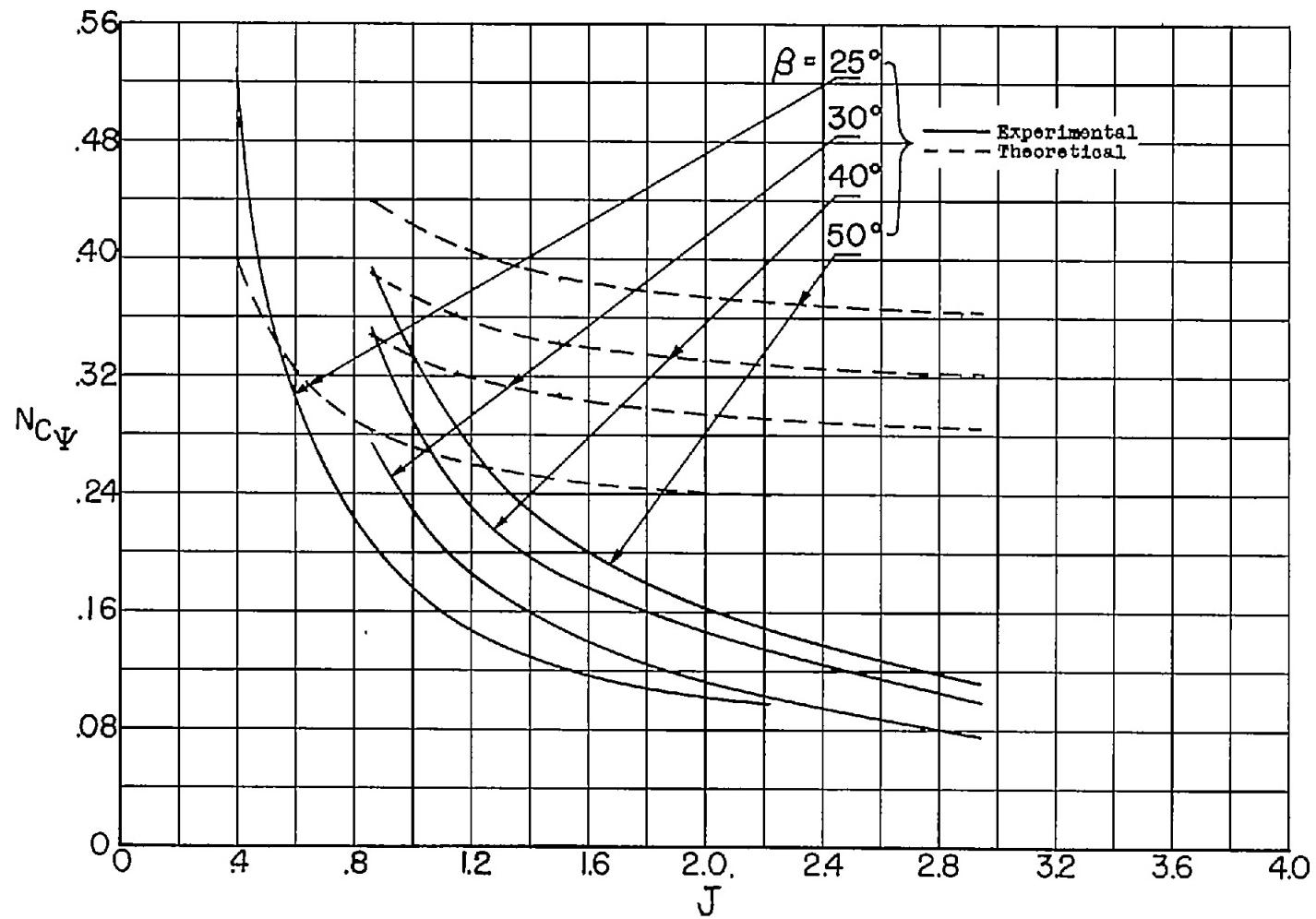
(d) $\alpha = 45°$.

Figure 19.- Continued.
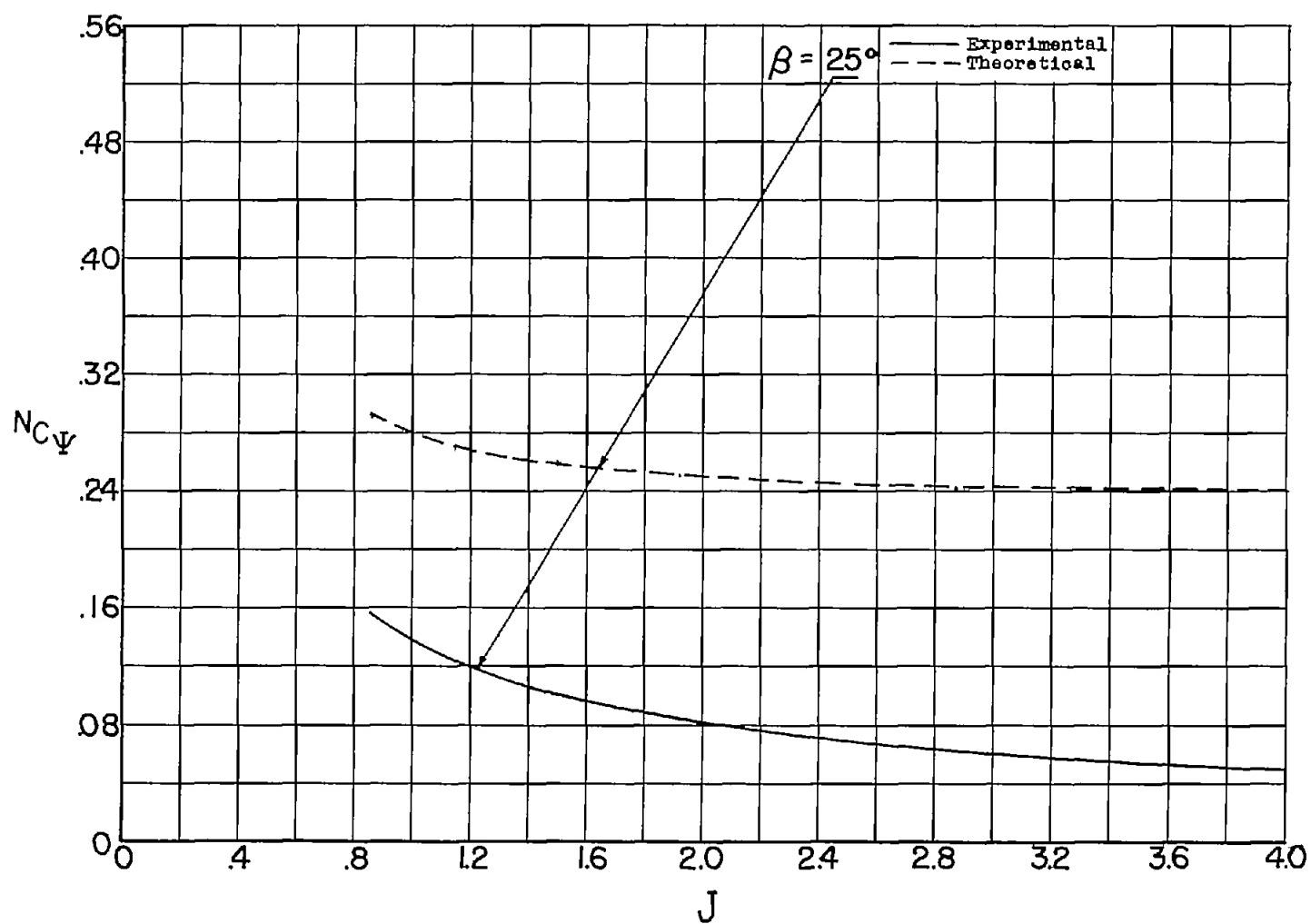
(e) $\alpha = 60°$.

Figure 19.- Continued.
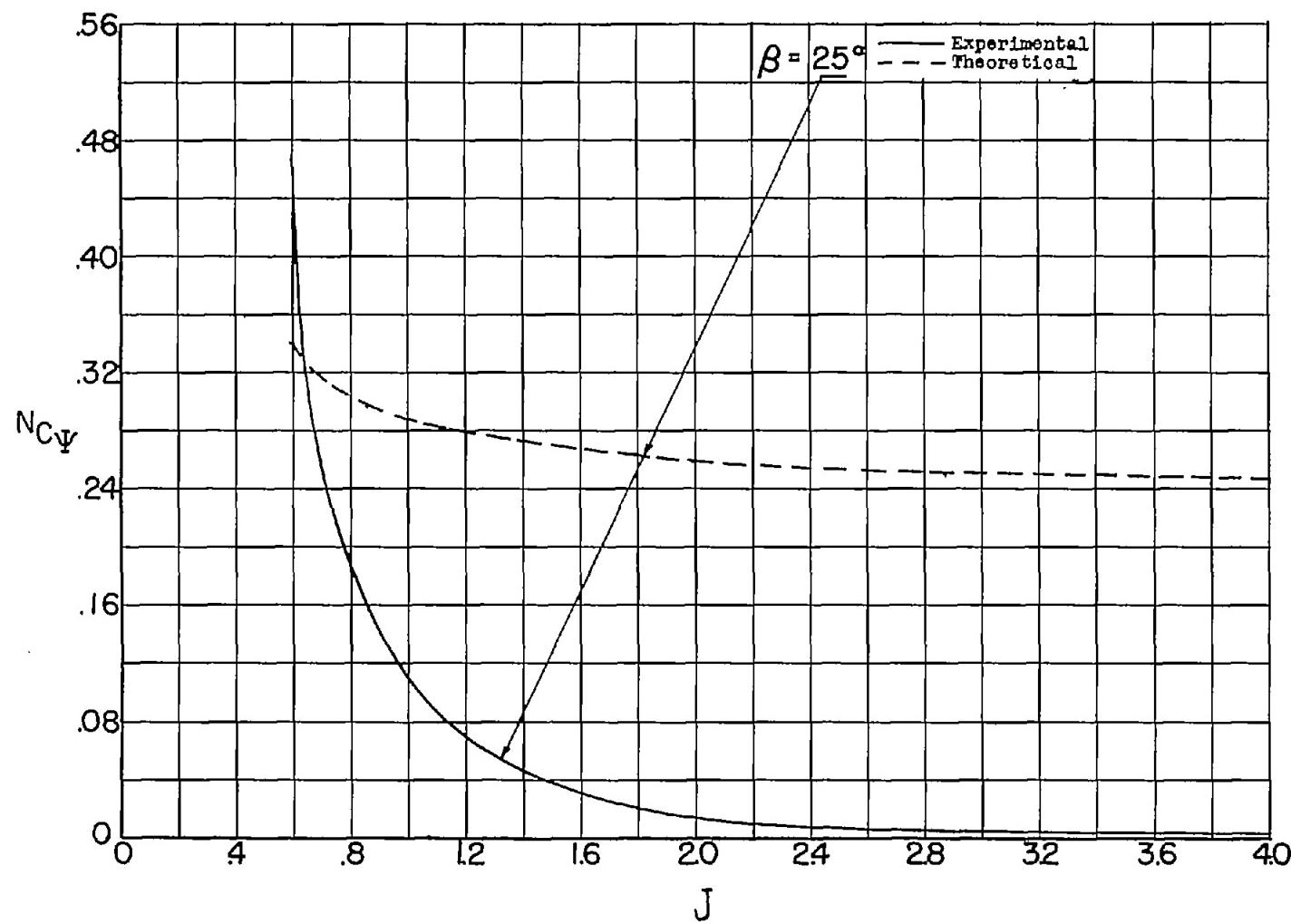
(f) $\alpha = 75°$.

Figure 19.- Continued.
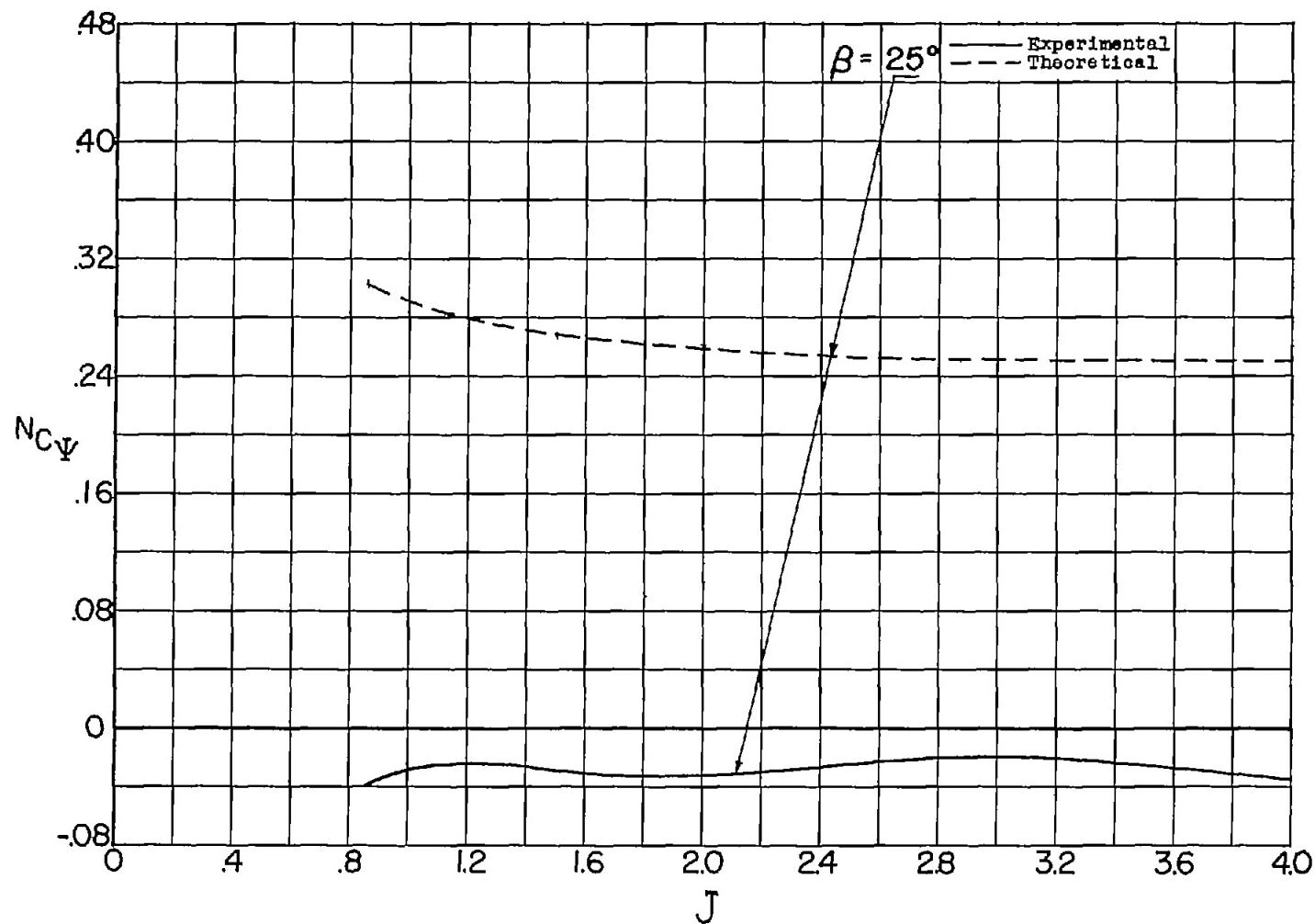
(g) α = 82.5°.

Figure 19.- Concluded.
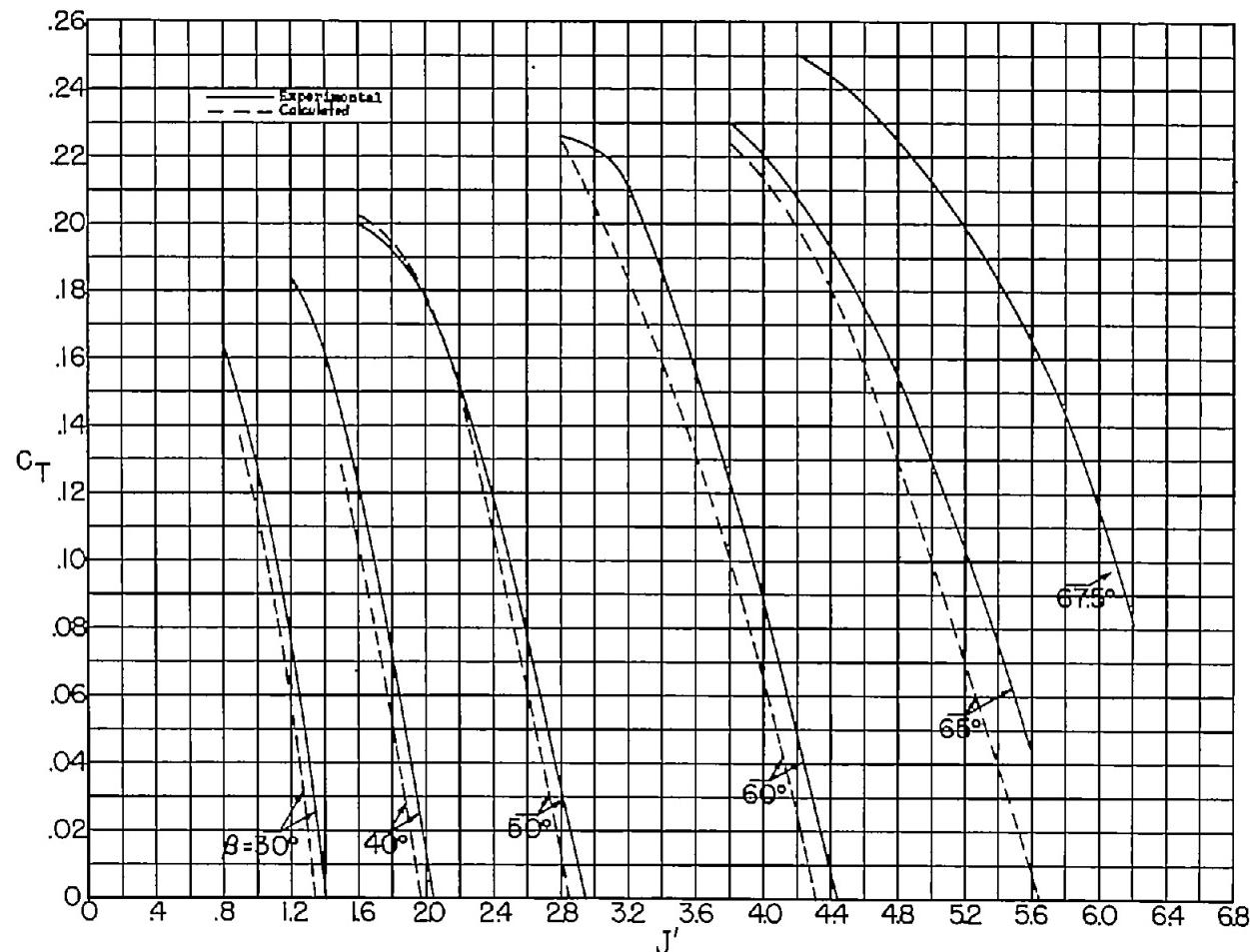
(a) C_T against J'.

Figure 20.- Comparison of experimental and calculated values of C_T, C_P, and η for a range of blade angle and advance ratio. $\alpha = 0°$.
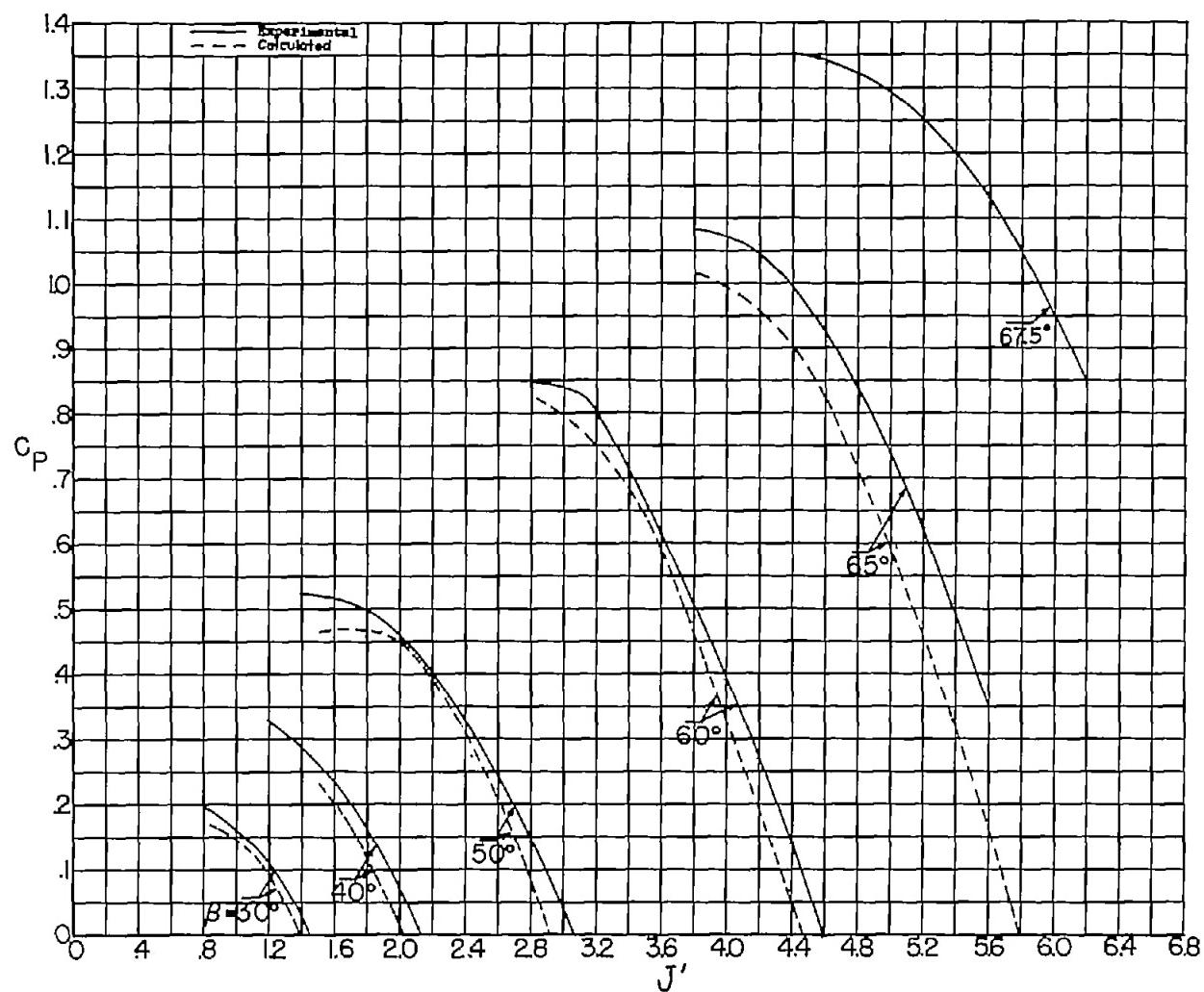
(b) C_P against J'.

Figure 20.- Continued.
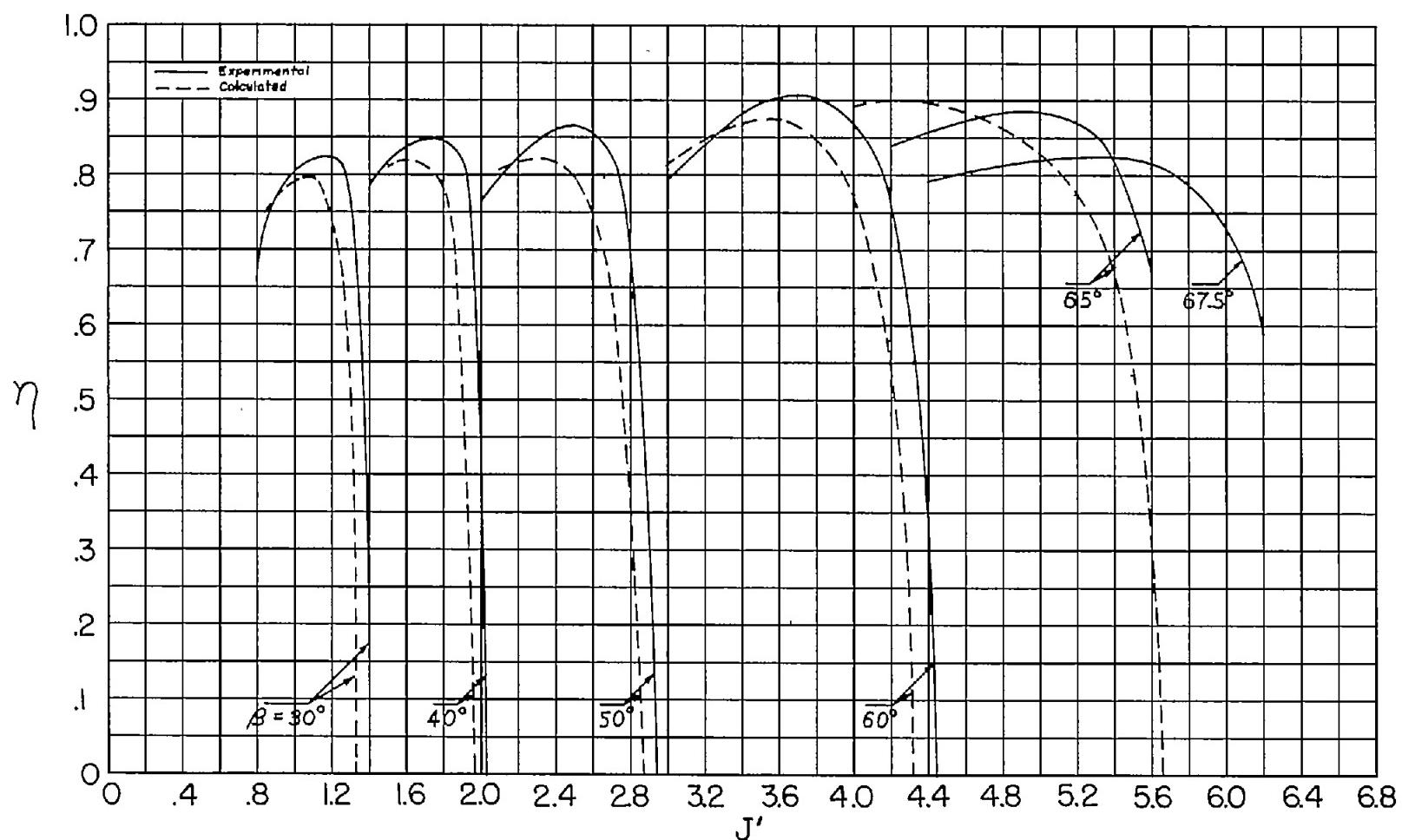
(c) η against J'.

Figure 20.- Concluded.